Article

Cell Reports

Functional and Molecular Characterization of Mechanoinsensitive "Silent" Nociceptors

Graphical Abstract

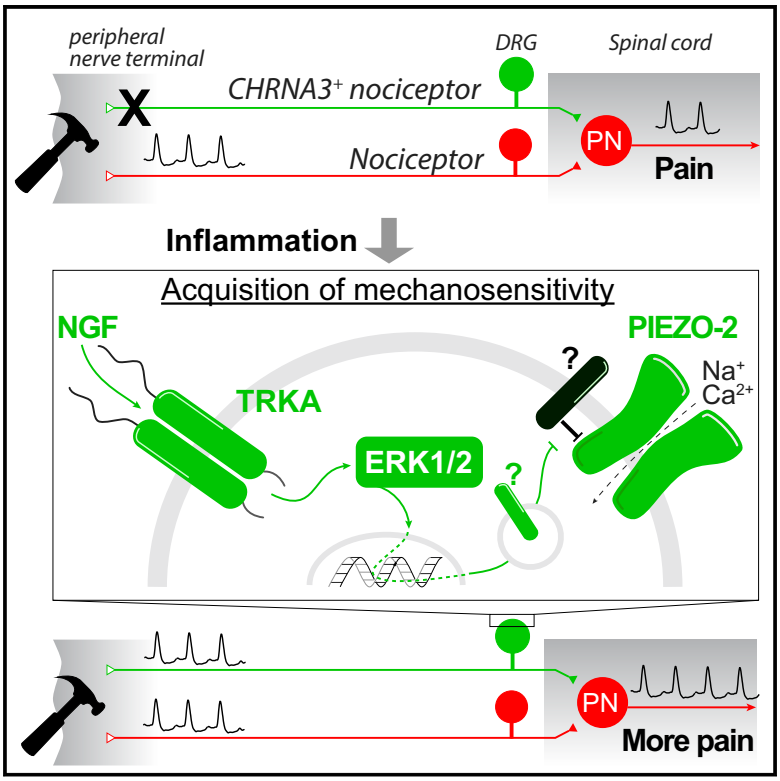

Authors

Vincenzo Prato, Francisco J. Taberner, James R.F. Hockley, ..., Paul A. Heppenstall, Ewan S. Smith, Stefan G. Lechner

Correspondence

stefan.lechner@pharma.uni-heidelberg.de

In Brief

Prato et al. find that mechanoinsensitive nociceptors account for ~50% of all nociceptors in visceral organs and deep somatic tissues and are sensitized to mechanical stimuli by the inflammatory mediator NGF, suggesting that they significantly contribute to inflammation-induced mechanical hyperalgesia.

Highlights

- A molecular marker for mechanoinsensitive "silent" nociceptors
- About 50% of all nociceptors in visceral organs and deep somatic tissues are "silent"
- NGF sensitizes silent, but not other, nociceptors to mechanical stimuli
- PIEZO2 is required for mechanosensitivity in silent nociceptors

Prato et al., 2017, Cell Reports *21*, 3102–3115
December 12, 2017
https://doi.org/10.1016/j.celrep.2017.11.066

CellPress

OPEN ACCESS
CellPress

Cell Reports
Article

Functional and Molecular Characterization of Mechanoinsensitive "Silent" Nociceptors

Vincenzo Prato,[1,4] Francisco J. Taberner,[1,2,4] James R.F. Hockley,[3] Gerard Callejo,[3] Alice Arcourt,[1] Bassim Tazir,[1] Leonie Hammer,[1] Paulina Schad,[1] Paul A. Heppenstall,[2] Ewan S. Smith,[3] and Stefan G. Lechner[1,5,*]

[1]Institute of Pharmacology, Heidelberg University, Im Neuenheimer Feld 366, 69120 Heidelberg, Germany
[2]EMBL Monterotondo, Via Ramarini 32, 00016 Monterotondo, Italy
[3]Department of Pharmacology, University of Cambridge, Tennis Court Road, Cambridge CB2 1PD, UK
[4]These authors contributed equally
[5]Lead Contact
*Correspondence: stefan.lechner@pharma.uni-heidelberg.de
https://doi.org/10.1016/j.celrep.2017.11.066

SUMMARY

Mechanical and thermal hyperalgesia (pain hypersensitivity) are cardinal signs of inflammation. Although the mechanism underlying thermal hyperalgesia is well understood, the cellular and molecular basis of mechanical hyperalgesia is poorly described. Here, we have identified a subset of peptidergic C-fiber nociceptors that are insensitive to noxious mechanical stimuli under normal conditions but become sensitized to such stimuli when exposed to the inflammatory mediator nerve growth factor (NGF). Strikingly, NGF did not affect mechanosensitivity of other nociceptors. We show that these mechanoinsensitive "silent" nociceptors are characterized by the expression of the nicotinic acetylcholine receptor subunit alpha-3 (CHRNA3) and that the mechanically gated ion channel PIEZO2 mediates NGF-induced mechanosensitivity in these neurons. Retrograde tracing revealed that CHRNA3$^+$ nociceptors account for ~50% of all peptidergic nociceptive afferents innervating visceral organs and deep somatic tissues. Hence, our data suggest that NGF-induced "un-silencing" of CHRNA3$^+$ nociceptors significantly contributes to the development of mechanical hyperalgesia during inflammation.

INTRODUCTION

The somatosensory nervous system comprises a remarkable variety of neurochemically and functionally diverse sensory afferents that enable us to detect and discriminate a wide range of tactile and noxious stimuli (Dubin and Patapoutian, 2010; Lechner and Lewin, 2013). Sensory neurons that are activated by noxious stimuli are termed nociceptors and are subclassified into unmyelinated C-fiber nociceptors and myelinated A-fiber nociceptors. The vast majority of all nociceptors are sensitive to mechanical stimuli, but various subpopulations with different sensitivities to additional noxious stimuli have been described in a wide variety of species. Nociceptors that are exclusively activated by mechanical stimuli are termed C-fiber and A-fiber mechanonociceptors; those that additionally respond to noxious thermal stimuli are collectively termed polymodal nociceptors but can be further subclassified according to their specific sensitivity to noxious heat and/or cold (Dubin and Patapoutian, 2010; Lewin and Moshourab, 2004).

The contribution of the various nociceptor subpopulations to different forms of acute pain is quite well understood. C-fiber nociceptors that express the heat-gated ion channel TRPV1, for example, are required for the detection of noxious heat and for the development of heat hyperalgesia (increased pain sensitivity to heat) (Brenneis et al., 2013; Cavanaugh et al., 2009), and one study also implicated TRPV1$^+$ afferents in the detection of noxious pinch stimuli (Brenneis et al., 2013). Moreover, it has been shown that noxious cold is detected by C-fiber nociceptors that express the cold- and menthol-sensitive ion channel TRPM8 (Knowlton et al., 2013). Last, whereas noxious mechanical stimuli applied with a blunt probe, such as a von Frey hair, are detected by C-fiber nociceptors that express the Mas-related G protein-coupled receptor D (Cavanaugh et al., 2009), sharp and potentially tissue damaging mechanical stimuli, such as a pinprick, are detected by a subset of A-fiber mechanonociceptors that are characterized by the expression of the neuropeptide Y receptor type 2 (Arcourt et al., 2017).

However, one subpopulation of nociceptors, the so-called silent nociceptors, has remained enigmatic ever since it was first described (Gold and Gebhart, 2010; Michaelis et al., 1996). The term "silent nociceptor" was originally introduced to describe sensory afferents that fired action potentials in response to electrical stimulation of the receptive field but could not be activated by physiologically relevant noxious mechanical stimuli. Silent nociceptors have been found in large numbers in the urinary bladder, the distal colon, and the knee joint (Feng and Gebhart, 2011; Gebhart, 1999; Häbler et al., 1990; Schaible and Schmidt, 1988) but are rare in rodent skin (Wetzel et al., 2007). In human skin, however, silent afferents account for almost one quarter of all C-fiber nociceptors (Schmidt et al., 1995). The fact that silent nociceptors are normally not activated by mechanical stimuli, suggests that they are not involved in mechanical pain signaling in healthy individuals. However, several studies have shown that silent afferents are sensitized to mechanical stimuli by a variety of compounds that are commonly used to experimentally induce inflammation, as well as by endogenous

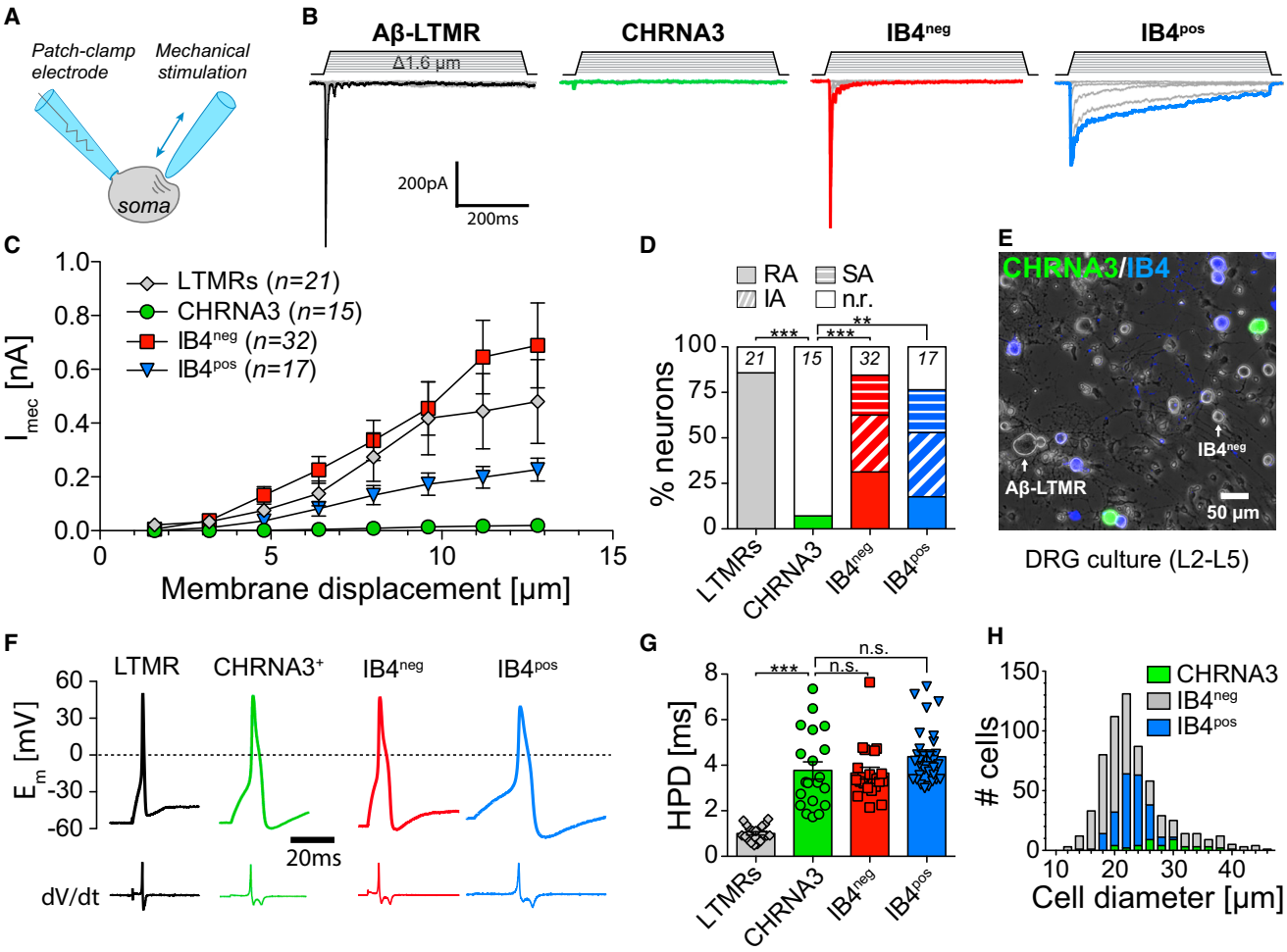

Figure 1. CHRNA3$^+$ Neurons Do Not Transduce Mechanical Stimuli into Electrical Signals

(A) Schematic illustration of the technique used to evoke and record mechanically activated currents.

(B) Example traces of whole-cell currents (bottom traces) evoked by mechanical stimulation (top traces) in the indicated cell types.

(C) The mean ± SEM peak mechanotransduction current amplitudes are shown as a function of membrane displacement.

(D) Comparison of the proportions of mechanoinsensitive (n.r.) and mechanosensitive neurons in the indicated sensory neuron subpopulations.

(E) Overlay of phase-contrast and fluorescence image of an IB4-labeled DRG culture from a CHRNA3-EGFP mouse.

(F) Typical AP of the indicated cell types (top traces). The bottom traces show the first derivative (dV/dt) of the AP, which exhibits two local minima if the AP has the nociceptor-specific hump in the falling phase.

(G) Comparison of the mean (bars) ± SEM (error bars) half-peak durations (HPDs) of the APs of the indicated cell types. The scattered symbols show the individual HPD values of each recorded cell. Kruskal-Wallis one-way ANOVA with Dunn's multiple-comparison test.

(H) Size distribution histogram of cultured DRG neurons showing that CHRNA3$^+$ neurons have medium cell diameters.

inflammatory mediators such as nerve growth factor (NGF) (Feng et al., 2012; Gold and Gebhart, 2010; Hirth et al., 2013; Schaible and Schmidt, 1985). Considering the large proportion of mechanically insensitive afferents in the aforementioned tissues, it is conceivable that un-silencing them would greatly increase nociceptive input to pain processing circuits in the spinal cord and higher brain regions. Accordingly it has been proposed that silent afferents may significantly contribute to mechanical hyperalgesia during inflammation (Gold and Gebhart, 2010). However, because of the lack of molecular markers that would allow the unequivocal identification or the selective functional manipulation of silent afferents, this hypothesis has never been directly tested. Moreover, the molecular mechanism that mediates the un-silencing of silent nociceptors has not yet been described.

RESULTS

CHRNA3$^+$ Sensory Neurons Are Mechanoinsensitive Peptidergic C-Fiber Nociceptors

Mechanosensitivity of dorsal root ganglion (DRG) sensory neurons is usually examined using the patch-clamp technique by recording whole-cell transmembrane currents evoked by mechanical stimulation of the cell soma (Figure 1A). In DRG neurons, three types of mechanically activated currents, which differ in their inactivation kinetics and were thus termed rapidly

adapting (RA), intermediately adapting (IA), and slowly adapting (SA) currents, have been described (Drew et al., 2002; Hu and Lewin, 2006; McCarter et al., 1999; Ranade et al., 2014). The ion channel PIEZO2 mediates the RA current in low-threshold mechanoreceptors (LTMRs), which detect tactile stimuli, but the mechanically gated channel required for mechanotransduction in nociceptors is still unknown (Ranade et al., 2014; Schrenk-Siemens et al., 2015). While we were screening several reporter mouse lines with the original goal of testing whether IA and SA currents are confined to genetically defined subsets of nociceptors, we made the observation that neurons in which EGFP is expressed under the control of the promoter of the nicotinic acetylcholine receptor subunit alpha-3 (CHRNA3) do not respond to mechanical stimuli at all. Thus only 1 of 15 tested CHRNA3$^+$ cells exhibited a tiny inward current in response to mechanical stimulation of the soma (Figures 1B–1D). In contrast, the majority of peptidergic C-fiber nociceptors (27 of 32 tested neurons), non-peptidergic nociceptors (13 of 17), and LTMRs (18 of 21) exhibited large mechanically evoked inward currents (Figures 1B–1D), which was consistent with previously published data (Drew et al., 2002; Hu and Lewin, 2006; Ranade et al., 2014). In these recordings, LTMRs and nociceptors were distinguished by means of cell size as well as action potential (AP) shape and duration, as previously described (Fang et al., 2005; Koerber et al., 1988). Peptidergic and non-peptidergic nociceptors were further discriminated by isolectin B4 (IB4) labeling, which specifically binds to non-peptidergic nociceptors (Figure 1E) (Molliver et al., 1997). Thus, small-diameter IB4-negative neurons with wide APs that exhibited the nociceptor-specific hump in the falling phase were classified as peptidergic C-fiber nociceptors, and large-diameter neurons with narrow uninflected spikes were classified as LTMRs (Figures 1E–1G). CHRNA3$^+$ neurons exhibited APs that were indistinguishable from those of other nociceptors but were significantly different from the APs of LTMRs (Figures 1F and 1G). Moreover, CHRNA3$^+$ neurons were not labeled by IB4 (Figure 1E), had small to medium-size cell bodies, and accounted for 7.8% ± 1.6% (n = 636) of the total population in cultures of L2–L5 DRGs (Figure 1H). To test if CHRNA3$^+$ neurons, as suggested by their AP configuration, are indeed nociceptors, we next examined the expression of well-established nociceptor subpopulation markers in CHRNA3$^+$ neurons in L3–L5 DRGs (Figures 2A–2D). The great majority of CHRNA3$^+$ neurons expressed the NGF receptor TRKA (94.6% ± 4.1%; Figures 2A and 2D) and the calcitonin gene-related peptide (CGRP) (90.5% ± 2.5%; Figures 2C and 2D), which are markers for peptidergic nociceptors (Averill et al., 1995), but did not express the glial cell line-derived neurotrophic factor (GDNF) receptor RET (1.8% ± 3.0%; Figures 2B and 2D), which is present in non-peptidergic neurons (Molliver et al., 1997). Moreover, only a few CHRNA3$^+$ neurons showed immunoreactivity for neurofilament heavy polypeptide (NEFH) (11.6% ± 5.4%; Figures 2A and 2D), which is expressed only in myelinated sensory neurons. The central projections of CHRNA3$^+$ neurons predominantly terminated in lamina I of the dorsal horn of the spinal cord, which is also characteristic of peptidergic nociceptors (Figure 2E). We also observed EGFP immunoreactivity in local neurons in lamina II$_o$ of the dorsal horn and scattered throughout lamina III. However, unlike the EGFP signals in lamina I, the signals in deeper laminae did not overlap with CGRP immunofluorescence (see insets in Figure 2E) and thus unlikely originate from CHRNA3$^+$ sensory afferents. Hence the electrophysiological data together with the immunohistochemical analysis strongly suggest that CHRNA3$^+$ neurons are mechanically insensitive, "silent," peptidergic C-fiber nociceptors.

CHRNA3$^+$ Neurons Densely Innervate Deep Somatic Tissues and Viscera but Are Absent from the Skin

Silent nociceptors have originally not only been found in the knee joint (Schaible and Schmidt, 1985), which is innervated by L3–L4 DRG neurons that we had investigated so far, but were shown to be even more abundant in visceral organs (Michaelis et al., 1996). Hence we next examined CHRNA3 expression in other spinal segments. Indeed, CHRNA3$^+$ neurons were present in all DRGs from cervical (C1) to sacral (S1), and almost all of them expressed CGRP (Figures 2F and S1A). More important, this analysis revealed that CHRNA3$^+$ neurons are rather rare in most DRGs (~15% of all CGRP$^+$ neurons) but account for up to 40% of the CGRP$^+$ population in thoracolumbar (T12–L1) and lumbosacral (L6–S1) DRGs (Figures 2F and 2G). This finding strongly supports our hypothesis that CHRNA3$^+$ neurons are silent nociceptors, because these DRGs give rise to the lumbar splanchnic nerve and the pelvic nerve, which innervate the colon and the bladder, where silent afferents have been found in large numbers (Christianson et al., 2007; Michaelis et al., 1996). While analyzing the immunolabeled sections, we noticed the presence of numerous neurons with extremely bright GFP fluorescence in lumbosacral DRGs (Figures 2F and S1B). Indeed, the GFP intensity distributions in L6–S1 DRGs and in T12–L1 DRGs were best fit with the sum of two Gaussians, whereas they were better fitted with a single Gaussian in all other DRGs, suggesting that two different populations of CHRNA3$^+$ neurons that significantly differ in their GFP intensities (hereafter termed GFP^{low} and GFP^{high} neurons) are present in thoracolumbar and lumbosacral DRGs (Figure S1C). GFP^{low} neurons had significantly higher levels of CGRP compared with GFP^{high} neurons (Figure S1D), suggesting that these two populations may also differ in their functional properties. To test this hypothesis, we examined the mechanosensitivity of the two populations in various spinal segments. GFP^{low} neurons from all spinal segments as well as GFP^{high} neurons from the thoracolumbar region were insensitive to mechanical stimuli, whereas GFP^{high} neurons from lumbosacral DRGs exhibited large mechanotransduction currents (Figures S2A and S2B). Hence, unless otherwise stated, hereafter the term "CHRNA3$^+$ neurons" refers to the mechanoinsensitive GFP^{low} population.

We next examined the peripheral projections of CHRNA3$^+$ neurons (Figures 3A–3F). In the distal colon and the urinary bladder, CHRNA3$^+$ fibers accounted for 92.1% ± 0.8% and 81.1% ± 0.5% of all CGRP$^+$ fibers, respectively (Figures 3B, 3C, and 3F). Moreover, we observed numerous CHRNA3$^+$ afferents in the knee joint (63.2 ± 0.7% of CGRP$^+$ fibers; Figures 3D and 3F) and the gastrocnemius muscle (62.5% ± 2.3% of CGRP$^+$ fibers; Figures 3E and 3F), but we did not find any CHRNA3$^+$ fibers in the glabrous and hairy skin (Figures 3A and S3A). Some sympathetic neurons, which also innervate the

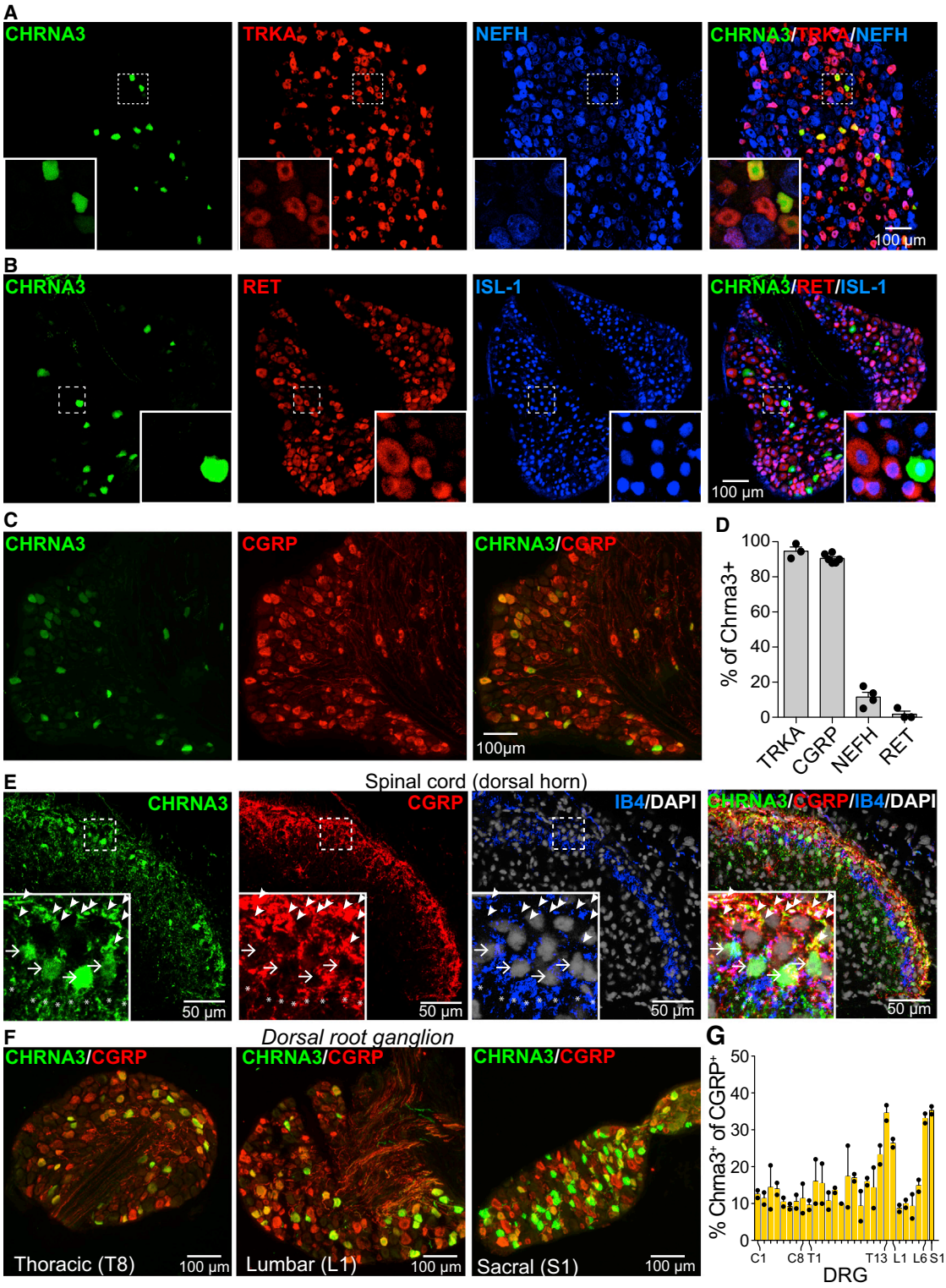

Figure 2. CHRNA3$^+$ Neurons Are Peptidergic C-Fiber Nociceptors

(A–C) Immunostaining of L3–L5 DRGs showing that CHRNA3$^+$ neurons express the peptidergic nociceptor markers TRKA (A) and CGRP (C) but not NEFH (A) and RET (B).

(D) Mean ± SEM percentage of CHRNA3$^+$ neurons that express the indicated marker protein. (N = 3–6 DRGs from two different mice; individual data points from each mouse are shown as black circles.)

(legend continued on next page)

examined tissues, also expressed CHRNA3. However, these cells did not express CGRP (Figures S3B and S3C), supporting the hypothesis that the CHRNA3$^+$/CGRP$^+$ fibers shown in Figures 3B–3E indeed originate from CHRNA3$^+$ sensory neurons. Heterogeneity in the GFP intensities, as observed in DRG stainings (Figures 2F, S1B, and S1C), was not evident in stainings of the bladder and the colon. Hence, to clarify whether the observed CHRNA3$^+$ fibers originated from GFP^{low} or GFP^{high} neurons, we next labeled sensory neurons that innervate the bladder and the colon with the retrograde tracer fast blue (FB) (Figures 4A and 4B). In T13 DRGs, 39.1% ± 3.2% of the CGRP$^+$ neurons that innervate the colon were GFP^{low}, whereas fewer than 10% were GFP^{high}. By contrast in S1 DRGs, both GFP^{low} (55% ± 6% of FB$^+$/CGRP$^+$ neurons) and GFP^{high} (37.2% ± 14.4%) neurons were labeled by FB injection into the colon (Figures 4A, 4D, and 4E). Similar results were obtained for the bladder, where FB injection labeled both GFP^{low} (40.5% ± 4.9%) and GFP^{high} (41.2% ± 0.7%) neurons in S1 DRGs but almost exclusively GFP^{low} cells (36.1% ± 12.7%) in T13 DRGs (Figures 4B and 4F). We also labeled knee joint afferents, which predominantly originate from L3 and L4 DRGs (da Silva Serra et al., 2016). Consistent with our previous results (Figure 3F), 56.2% ± 15.4% and 42.1% ± 10.7% of the FB$^+$/CGRP$^+$ neurons in L4 and L3 DRGs, respectively, were CHRNA3 positive (Figures 4C and 4G).

Hence, taken together, our data demonstrate that mechanoinsensitive CHRNA3$^+$ sensory neurons account for approximately half of all peptidergic nociceptors in tissues previously shown to be densely innervated by silent afferents (Feng and Gebhart, 2011; Gebhart, 1999; Häbler et al., 1990; Schaible and Schmidt, 1988).

CHRNA3$^+$ Neurons Are Sensitized to Mechanical Stimuli by NGF

A key feature of silent nociceptors is their ability to become sensitized to mechanical stimuli by inflammatory mediators. We thus next asked if CHRNA3$^+$ (GFP^{low} from L2–L5 DRGs) neurons acquire mechanosensitivity after treatment with NGF (50 ng/mL) or an inflammatory soup containing 10 μM bradykinin, 10 μM prostaglandin E_2, 10 μM histamine, and 10 μM serotonin. One hour treatment with NGF or the inflammatory soup did not affect mechanosensitivity of CHRNA3$^+$ neurons (Figures 5A–5C and S4; note that both treatments were applied after the cells had been cultured in normal growth medium for 24 hr). After 24 hr treatment with NGF, however, CHRNA3$^+$ neurons acquired mechanosensitivity and responded to mechanical stimulation with large inward currents, which did not further increase when NGF and inflammatory soup were applied together (Figures 5A–5C and S4). Interestingly, NGF did not modulate the amplitude or the kinetics of mechanotransduction currents in small-diameter IB4-negative neurons, that is, putative TRKA-expressing peptidergic C-fiber nociceptors (Figures 5D–5F). Inflammatory soup alone also had no effect on mechanosensitivity of IB4-negative neurons. However, after 24 hr treatment with NGF, 1 hr treatment with the inflammatory soup caused a small but significant increase of mechanotransduction current amplitudes elicited by small membrane displacements (Figure 5E), as well as a slowing of inactivation kinetics (Figure 5F).

Via binding to the TRKA receptor, NGF can activate multiple signaling pathways, including the PLCγ pathway, the PI3-kinase pathway, and the Ras/Raf/MEK/ERK pathway (Denk et al., 2017). To examine which of these signaling pathways mediated the sensitization of CHRNA3$^+$ neurons, we next incubated DRG cultures for 24 hr with NGF in the presence of 5 μM U73122, a PLCγ blocker, 500 nM wortmannin (WTM), a PI3-kinase blocker, or 10 μM U0126, an ERK1/2 blocker (Figure 6A). U73122 and WTM did not alter the effect of NGF treatment, but CHRNA3$^+$ neurons treated with U0126 exhibited significantly smaller mechanotransduction currents than neurons from the same cultures treated with NGF alone (Figure 6B). ERK1/2 kinases can regulate gene transcription but can also directly modulate ion channels by phosphorylation. To test if the former mechanism is involved, we incubated CHRNA3$^+$ neurons for 24 hr with NGF in the presence of the transcription blocker actinomycin D (2 μg/mL). Indeed, mechanotransduction currents were significantly smaller when cultures were treated with actinomycin D (Figure 6B), suggesting that *de novo* gene transcription is required for the NGF-induced acquisition of mechanosensitivity in CHRNA3$^+$ neurons.

We next sought to identify the ion channel that confers mechanosensitivity on CHRNA3$^+$ neurons. In LTMRs, RA-type mechanotransduction currents are mediated by PIEZO2, but the ion channel that mediates mechanotransduction currents in nociceptors is still unknown (Ranade et al., 2014). Several proteins have been implicated in mechanosensitivity of sensory neurons such as the acid-sensing ion channels ASIC2 and ASIC3 (Price et al., 2000, 2001), the transient receptor potential channels TRPA1 (Vilceanu and Stucky, 2010), TRPC3 and TRPC6 (Quick et al., 2012) and TMEM150c (Hong et al., 2016), but conflicting results have been published regarding their precise role in mechanotransduction (Drew et al., 2004; Dubin et al., 2017). To test if any of these putative mechanotransduction genes was present in CHRNA3$^+$ neurons and upregulated by NGF, we next compared their mRNA levels in CHRNA3$^+$ neurons from L2–L5 DRGs cultured for 24 hr in the presence and absence of NGF using qPCR (Figure 7A). This analysis showed that transcripts for none of these proteins were upregulated by NGF. Unexpectedly, however, the qPCR data revealed that even under

(E) CHRNA3$^+$ fibers project to lamina I, which was visualized with CGRP staining. CHRNA3$^+$ fibers in lamina IIo (IB4-positive) and below were CGRP negative (compare signals marked by arrowheads and asterisks in the inset) and hence likely originate from the CHRNA3$^+$/CGRP$^-$ local neurons in lamina II (cells marked with arrows).

(F) Representative images showing co-expression of CHRNA3 and CGRP in thoracic, lumbar, and sacral DRGs. In sacral DRGs, numerous neurons exhibit particularly bright CHRNA3 immunofluorescence. For a detailed analysis of the neurochemical and electrophysiological differences between bright and less bright CHRNA3$^+$ neurons, see Figures S1 and S2.

(G) Overview of the proportions of CGRP$^+$ neurons that express CHRNA3 in the indicated DRGs (C, cervical; T, thoracic; L, lumbar; S, sacral). Bars represent mean ± SEM (N = 2 mice, percentage of individual mice are shown as black circles).

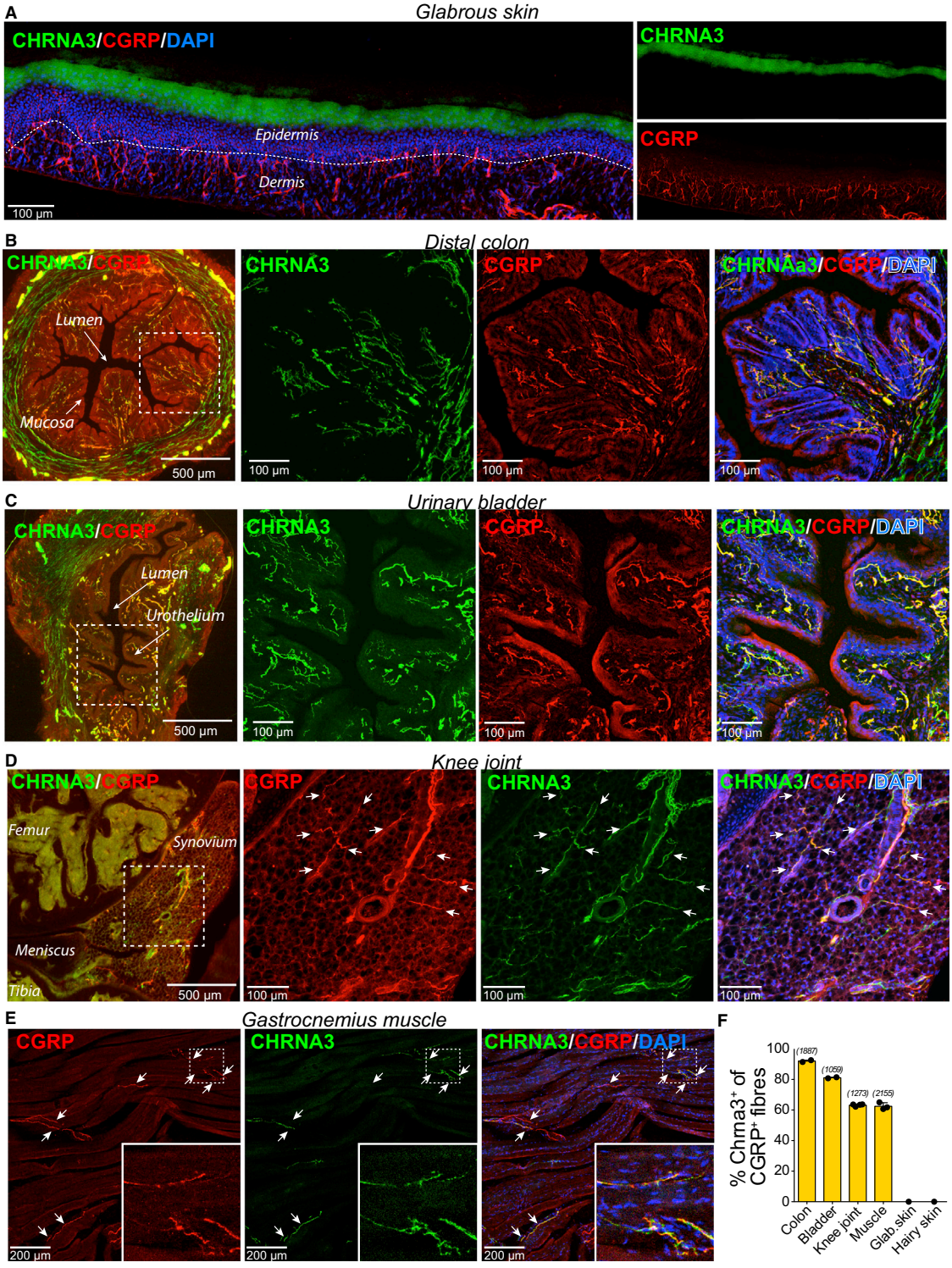

Figure 3. Peripheral Projections of CHRNA3$^+$ Neurons

(A–E) Immunostainings of tissue sections of the glabrous skin (A), the distal colon (B), the urinary bladder (C), the knee joint (D), and the gastrocnemius muscle (E) to visualize innervation by CHRNA3$^+$/CGRP$^+$ sensory afferents. Also see Figure S3. Images shown in (A) are composite images assembled from multiple high-resolution images. The three images on the right in (B)–(D) show magnified views of the regions marked with the dashed white squares in the leftmost images. (F) Quantification of the proportion of CGRP$^+$ fiber fragments (i.e., each connected fluorescent entity was considered as a fiber fragment) that express CHRNA3. Bars represent mean ± SEM (N = 2–4 mice; individual data points from each mouse are shown as black circles).

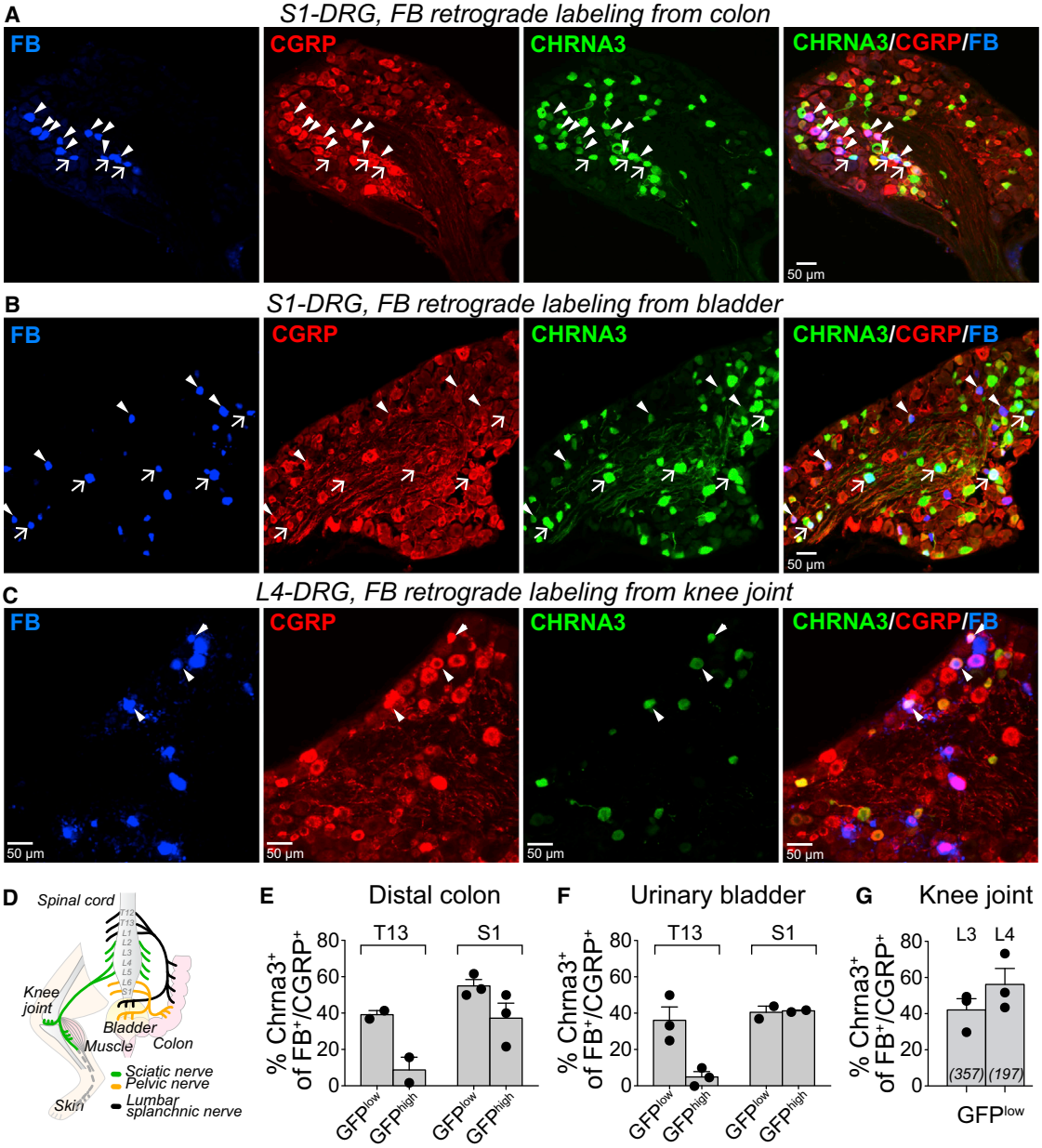

Figure 4. Retrograde Labeling of Sensory Afferents Innervating the Colon, the Bladder, and the Knee Joint

(A–C) Representative images of DRG neurons retrogradely labeled with fast blue (FB) from the colon (A), the bladder (B), and the knee joint (C) and co-stained for CHRNA3 and CGRP. Arrowheads in (A)–(C) mark GFP^{low}-CHRNA3^{+} neurons, and arrows mark GFP^{high}-CHRNA3^{+} neurons.

(D) Schematic illustration of the origin of sensory afferents that innervate the colon, the bladder, the knee joint, and the gastrocnemius muscle.

(E–G) Quantification of the percentage of CHRNA3^{+}-GFP^{low} (mechanoinsensitive) and CHRNA3^{+}-GFP^{high} (mechanosensitive) among FB^{+}/CGRP^{+} in T13, S1, and L3–L4 DRGs, that is, among CGRP^{+} afferents that innervate the colon (E), the bladder (F), and the knee joint (G). Bars represent mean ± SEM (N = 2 or 3 mice; proportions of individual mice are shown as black circles). Note that CHRNA3-GFP^{low} (mechanoinsensitive) afferents account for ~50% of all CGRP^{+} afferents in the bladder, colon, and knee joint.

control conditions, CHRNA3^{+} neurons express PIEZO2 at levels comparable with those in LTMRs. The presence of PIEZO2 was further confirmed by immunolabeling of L2–L5 DRGs, which showed that 94.9% (278 of 293) of the CHRNA3^{+} neurons express PIEZO2 (Figure 7B), suggesting that mechanotransduction currents in CHRNA3^{+} neurons are indeed mediated by PIEZO2. This hypothesis was supported by additional electrophysiological experiments showing that similar to PIEZO2-mediated currents (Coste et al., 2010), mechanotransduction currents in CHRNA3^{+} neurons reversed at close to 0 mV and exhibited

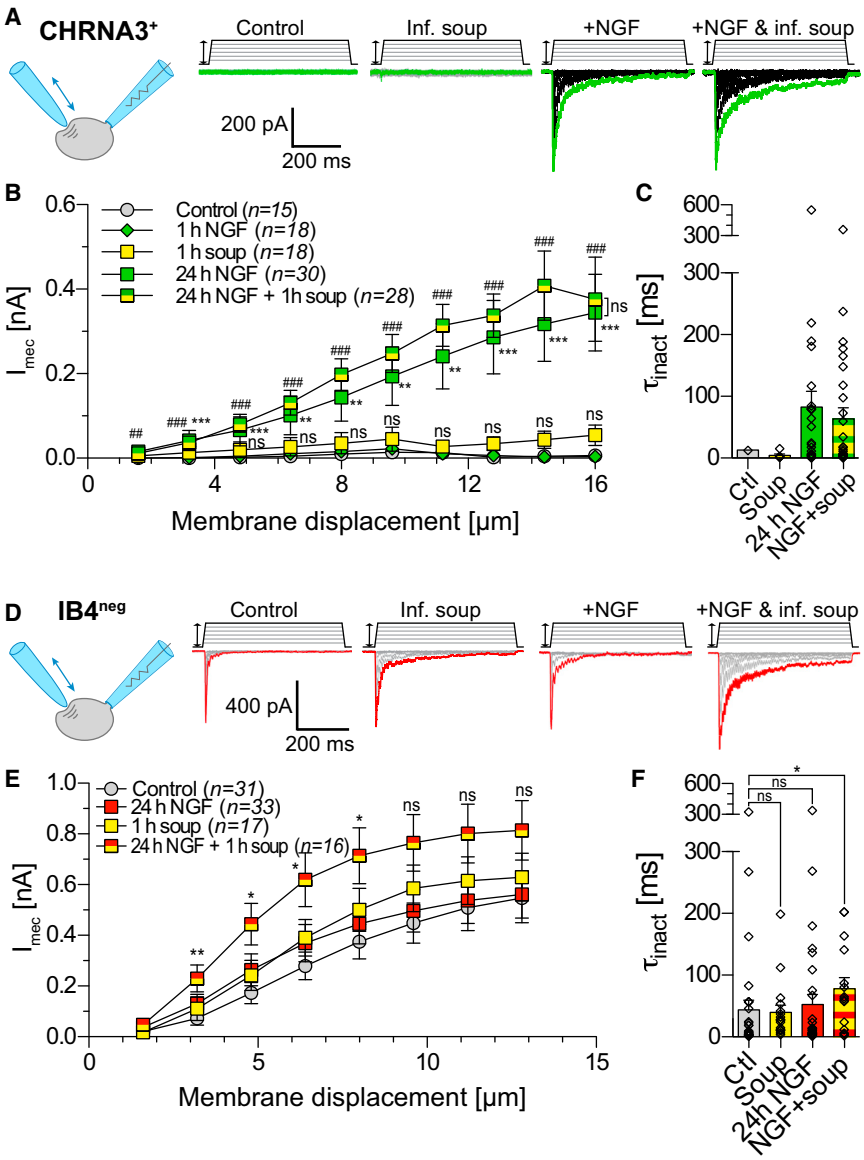

Figure 5. NGF Sensitizes CHRNA3$^+$ Neurons but Not IB4^{neg} Neurons to Mechanical Stimuli

(A) Representative example traces of whole-cell currents (bottom traces) evoked by mechanical stimulation (top traces) in CHRNA3$^+$ neurons cultured for 24 hr in normal growth medium (control), for 24 hr in growth medium + 1 hr inflammatory soup before recording (inf. soup), after 24 hr treatment with 50 ng/mL NGF (+NGF), and after 24 hr NGF + 1 hr inflammatory soup.

(B) Comparison of the displacement-response curves of CHRNA3$^+$ neurons after the indicated treatments (data points represent mean ± SEM mechanotransduction current amplitudes). Current amplitudes evoked by the same membrane displacement in the different conditions were compared using Kruskal-Wallis one-way ANOVA and Dunn's multiple-comparison test. The p values of Dunn's multiple-comparison test are indicated by asterisks for control versus 24 hr NGF and by a pound sign for control versus 24 hr NGF + 1 hr soup.

(C) Comparison of the inactivation time constants (τ_{inact}) of the mechanotransduction currents recorded in the indicated conditions. Bars represent mean ± SEM τ_{inact}. Individual data points from which the means were calculated are shown in the aligned dot plot. Also see Figure S4.

(D–F) Same parameters as in (A)–(C) but for mechanotransduction currents evoked in small diameter IB4^{neg} neurons: (D) whole-cell currents, (E) displacement-response curves, and (F) inactivation time constants. Note that NGF neither modulates mechanotransduction current amplitudes nor inactivation kinetics.

DISCUSSION

Here, we have identified a molecular marker for mechanoinsensitive "silent" nociceptors. We show that sensory neurons that express CHRNA3 constitute a subset of peptidergic C-fiber nociceptors that are completely insensitive to mechanical stimuli under normal conditions but become sensitized to such stimuli when exposed to the inflammatory mediator NGF. Strikingly, the mechanosensitivity of other nociceptors does not appear to be affected by NGF treatment. We further show that the mechanically gated ion channel PIEZO2 mediates NGF-induced mechanosensitivity in CHRNA3$^+$ nociceptors. Because CHRNA3$^+$ afferents account for ~50% of all peptidergic nociceptors innervating visceral organs and deep somatic tissues, we propose that the NGF-induced un-silencing of CHRNA3$^+$ afferents significantly contributes to the development of mechanical hyperalgesia during inflammation.

significantly slower inactivation kinetics at positive membrane potentials (Figures 7C–7E). Moreover, mechanotransduction currents in CHRNA3$^+$ neurons were inhibited by the toxin GsMTx4 (Figure 7F), which had been shown to block PIEZO2 currents (Wang et al., 2017). Finally, small interfering RNA (siRNA)-mediated knockdown of PIEZO2 expression in CHRNA3$^+$ neurons prevented the acquisition of mechanosensitivity in NGF-treated cells (Figures 7G and 7H).

In summary, our data show that PIEZO2 confers mechanosensitivity to CHRNA3$^+$ neurons. However, because PIEZO2 is also expressed in the absence of NGF (i.e., under conditions in which CHRNA3$^+$ neurons do not exhibit mechanotransduction currents) our data further suggest that PIEZO2 is normally inhibited in these cells and is released from this inhibition by NGF-induced upregulation of a yet unidentified protein (Figure 7I).

The Contribution of CHRNA3$^+$ Neurons to Inflammation-Induced Mechanical Hyperalgesia

NGF plays an important role in the induction and maintenance of pain hypersensitivity associated with inflammation (Denk et al.,

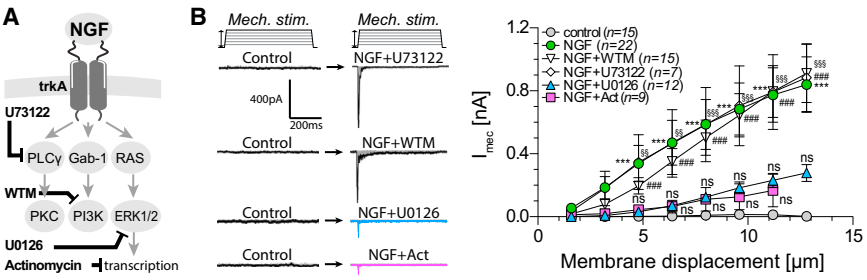

Figure 6. The Acquisition of Mechanosensitivity Requires *De Novo* Gene Transcription

(A) Schematic illustration of the intracellular signaling cascades activated by NGF.

(B) Example traces (left) and displacement-response curves (right) of mechanotransduction currents of CHRNA3$^+$ neurons treated with NGF and the indicated inhibitors of the signaling cascades shown in (A). Current amplitudes evoked by the same membrane displacement in the different conditions were compared using Kruskal-Wallis one-way ANOVA and Dunn's multiple-comparison test. The p values of Dunn's multiple-comparison test are indicated by asterisks for 24 hr NGF versus control, by pound signs for NGF + U73122 versus control, and by section signs for NGF + WTM versus control.

2017; Lewin et al., 2014), which is highlighted by several important observations. Thus, a single NGF injection induces profound and long-lasting thermal and mechanical hyperalgesia in rodents and humans (Dyck et al., 1997; Lewin et al., 1993; Rukwied et al., 2010). Moreover, sequestering endogenously produced NGF with anti-NGF antibodies blocks hyperalgesia associated with experimentally induced inflammation in rodents (Woolf et al., 1994) and, most important, alleviates pain in humans suffering from a variety of painful chronic inflammatory diseases (Chang et al., 2016; Denk et al., 2017). Although the mechanism underlying NGF-induced heat hyperalgesia is well understood, little is known about the cellular and molecular basis of mechanical hyperalgesia.

Our data suggest that CHRNA3$^+$ silent nociceptors may contribute to the development of inflammatory mechanical hyperalgesia in visceral organs, muscles, and joints, via the following mechanism: under normal conditions, CHRNA3$^+$ neurons are mechanoinsensitive (Figures 1A–1D), and hence noxious mechanical stimuli only activate other mechanosensitive nociceptors, leading to normal pain perception (Figure 7I). During inflammation, however, increased NGF levels in the inflamed tissues (Chen et al., 2016; Denk et al., 2017) lead to un-silencing of CHRNA3$^+$ afferents (Figures 5A–5C). Considering that silent afferents account for ~50% of all nociceptors in these tissues (Figure 4), the consequence of this un-silencing is that the number of nociceptive afferents that are activated by a given noxious mechanical stimulus is doubled, which inevitably results in significantly increased excitatory drive onto projection neurons in the spinal cord and hence to increased pain sensitivity (Figure 7I).

So is this model in accordance with previously published data and models regarding possible mechanisms of mechanical hyperalgesia? First, we would like to emphasize that we do not claim that the un-silencing of CHRNA3$^+$ afferent is the only mechanism underlying NGF-induced hyperalgesia. Our findings do not rule out a possible contribution of previously described mechanisms such as NGF-induced increases in the synthesis and release of brain-derived neurotrophic factor (BDNF) from the central synapses of nociceptors, which leads to strengthened synaptic transmission and hence amplified pain signaling, or NGF-induced changes in the electrical excitability of nociceptors resulting from subtle changes in the expression levels and the functional properties of the voltage-gated sodium channels Nav1.7 and Nav1.8 (Lewin et al., 2014; Pezet and McMahon, 2006). However, given the remarkable sensitivity to NGF (Figure 5) and the high incidence of CHRNA3$^+$ afferents in viscera and deep somatic tissues (Figures 3 and 4), it is tempting to speculate that the contribution of CHRNA3$^+$ afferents to pain hypersensitivity in these tissues is quite considerable. Indeed, there is compelling clinical evidence indicating that NGF-signaling plays a particularly important role in the development of pain hypersensitivity in the joints, in the bladder, and in muscles. Thus numerous clinical trials have demonstrated that anti-NGF therapy shows particularly great efficacy in alleviating pain associated with osteoarthritis, interstitial cystitis, and low back pain (Chang et al., 2016; Denk et al., 2017). Our observation that mechanoinsensitive CHRNA3$^+$ afferents account for approximately 50% of all peptidergic nociceptors in the colon, the bladder, the knee joint, and muscles (Figures 3 and 4) is consistent with previous electrophysiological studies, which found that the proportion of silent afferents among C-fiber nociceptors is between 30% and 90% in these tissues (Feng and Gebhart, 2011; Gebhart, 1999; Gold and Gebhart, 2010; Häbler et al., 1990; Michaelis et al., 1996; Schaible and Schmidt, 1985). Silent afferents have also been found in large numbers (~25%) in cutaneous nerves of humans and monkeys (Meyer et al., 1991; Schmidt et al., 1995), but they appear to be extremely rare (<10% of all C-fiber nociceptors) in the mouse skin (Wetzel et al., 2007). Hence, the absence of CHRNA3$^+$ afferents from both hairy and glabrous skin (Figures 3A and S3A) was not fully unexpected. It is unlikely that we overlooked CHRNA3$^+$ afferents innervating the skin, considering that we have analyzed a total of 120 skin sections from three different mice. Hence, we propose that silent cutaneous afferents are genetically different from those innervating the viscera and deep somatic tissues.

The Effects of NGF on Mechanosensitivity

Another important finding of our study was that NGF sensitizes only CHRNA3$^+$ neurons but not other TRKA-expressing nociceptors (IB4^{neg} neurons), to mechanical stimuli (Figure 5). At first glance, the finding that IB4^{neg} neurons are not sensitized to mechanical stimuli appears to contradict previous reports from others and us, showing that mechanotransduction currents in IB4^{neg} neurons are modulated by NGF (Di Castro et al., 2006; Lechner et al., 2009). In this context, it is important to note that here we have used adult animals (8–12 weeks old), whereas in our previous study, we examined neurons from newborn mice (Lechner et al., 2009), and Di Castro et al. (2006) studied juvenile

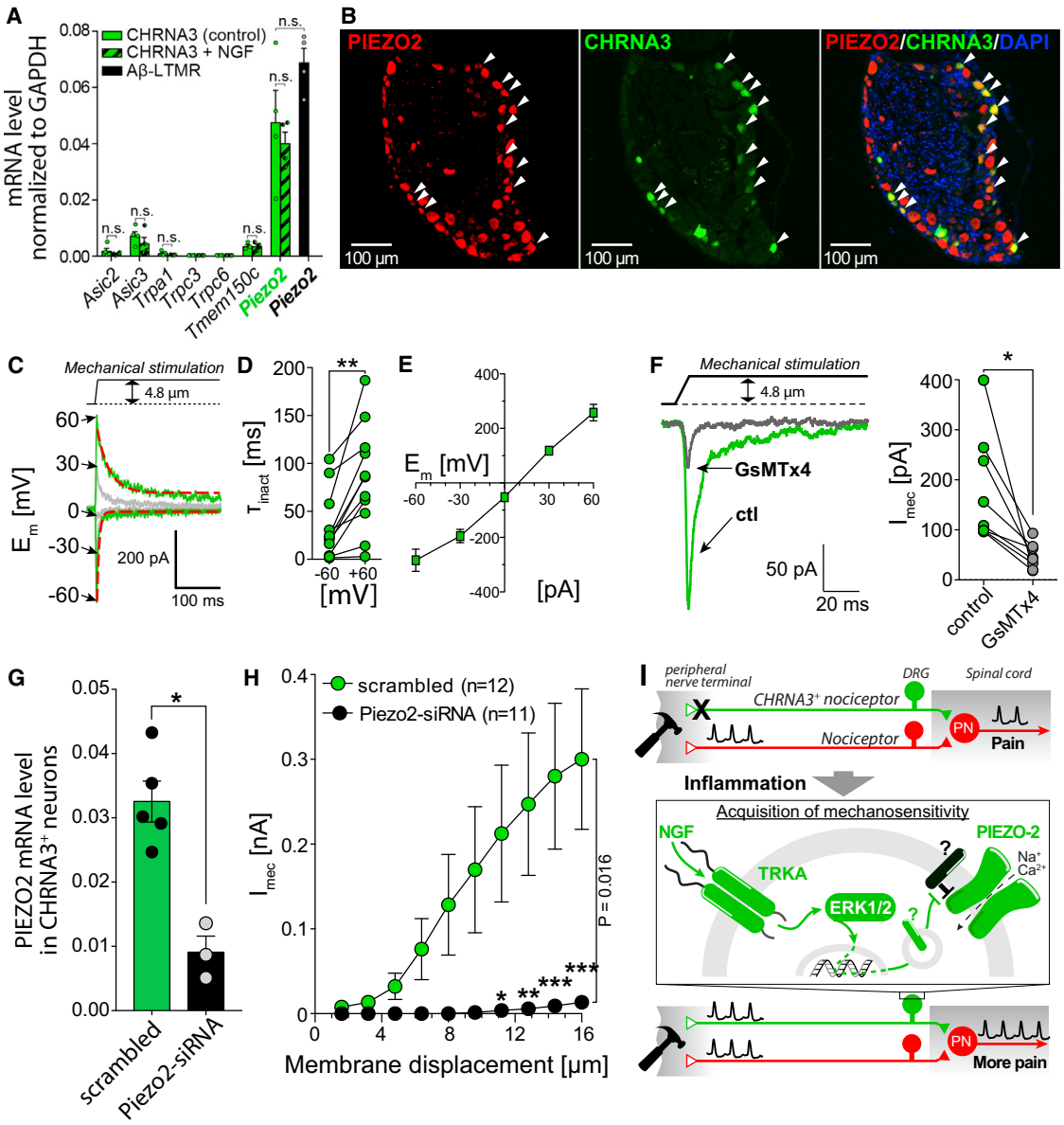

Figure 7. Mechanotransduction in CHRNA3$^+$ Neurons Requires PIEZO2

(A) Comparison of the expression levels of the indicated genes in CHRNA3$^+$ neurons under control conditions (green bars) and after 24 hr treatment with NGF (hatched bars). Note that under control conditions CHRNA3$^+$ neurons express Piezo2 at similar levels as Aβ-LTMRs (black bar). Bars represent mean ± SEM from three or four samples (one sample per mouse).

(B) Immunolabeling of an L4 DRG showing PIEZO2 expression in CHRNA3$^+$ neurons (marked by arrowheads).

(C) Example traces of mechanotransduction currents evoked by a 4.8 µm membrane displacement of a CHRNA3$^+$ neuron at the indicated membrane potentials. Inactivation was fitted with a single exponential function (red dashed line).

(D) Paired dot plot comparing inactivation time constants (τ_{inact}) of mechanotransduction currents at −60 mV and +60 mV. At +60 mV, currents inactivate significantly slower than at −60 mV (paired t test, p = 0.0012).

(E) I-V curve showing that mechanotransduction currents in CHRNA3$^+$ neurons after 24 hr NGF treatment reverse at around 0 mV, suggesting that they are mediated by a non-selective cation channel. Symbols represent mean ± SEM (n = 11).

(F) Example traces (left) and paired dot plot (right) showing that mechanotransduction currents in CHRNA3$^+$ neurons are inhibited by GsMTx4 (n = 8, paired t test, p = 0.0118).

(G) Comparison of the Piezo2 expression levels in CHRNA3$^+$ neurons transfected with non-targeting siRNA (scrambled) and Piezo2-siRNA, showing that Piezo2 expression was reduced by ~72% (0.032 ± 0.0031 versus 0.0091 ± 0.0025; Mann-Whitney test, p = 0.0357).

(H) Comparison of the displacement-response curves of NGF-treated CHRNA3$^+$ neurons transfected with non-targeting siRNA (green circles) and Piezo2-siRNA (black circles). Curves were compared using a two-way repeated-measures ANOVA (p = 0.016) with Bonferroni post-test.

(I) Model of the mechanism underlying the acquisition of mechanosensitivity and the possible contribution to increased pain sensitivity during inflammation.

rats. However, it is well known that NGF is important for the functional maturation of sensory neurons during embryonic and postnatal development of sensory neurons (Lewin et al., 2014; Luo et al., 2007). We have actually shown that NGF is required for the developmental acquisition of mechanosensitivity in IB4^{neg} neurons (Lechner et al., 2009). Moreover, it was shown that the diversification of nociceptors into peptidergic TRKA^{+} neurons and non-peptidergic TRKA^{-}/RET^{+} neurons is only completed 3 weeks after birth (Bennett et al., 1996; Molliver and Snider, 1997; Molliver et al., 1997). Hence NGF-dependent effects observed in newborn or juvenile animals should be interpreted with caution, as they might solely reflect incomplete maturation of nociceptors. Indeed, using extracellular single-unit recordings from the saphenous nerve, it was recently shown that in the complete Freund's adjuvant (CFA) model of inflammation, peripheral sensitization of cutaneous nociceptors occurs only in young but not in aged mice (Weyer et al., 2016). So does that mean that the mechanosensitivity of CHRNA3-negative peptidergic nociceptors is not at all altered during inflammation and that NGF does not in general modulate the functional properties of these neurons? Not quite. Although our data show that NGF does not directly modulate mechanotransduction currents in IB4^{neg} neurons, we demonstrate that an inflammatory soup potentiates mechanotransduction currents only after pretreatment with NGF (Figure 5E). A possible explanation for this observation is that NGF upregulates the expression of genes that are required for the actions of other inflammatory mediators. Indeed, it has been shown that the B2 receptor for bradykinin, which was present in the inflammatory soup used in this study, is upregulated in nociceptors by NGF (Lee et al., 2002). Moreover, Di Castro et al. (2006) showed that in juvenile rats, direct activation of protein kinase C with the phorbol ester PMA sensitizes mechanotransduction currents in IB4^{neg} neurons only after pretreatment with NGF. Hence, we conclude that in addition to inducing a complete phenotypic switch in CHRNA3^{+} neurons, NGF primes other peptidergic nociceptors for subsequent sensitization by other inflammatory mediators, which, however, have only moderate effects on mechanosensitivity.

The Molecular Basis of NGF-Induced Mechanosensitivity in CHRNA3^{+} Neurons

During the past two decades, numerous ion channels, such as ASIC channels, TRPA1, TRPC3, TRPC6, TMEM150c, and PIEZO2, have been proposed to contribute to mechanosensitivity of sensory neurons (Hong et al., 2016; Price et al., 2000, 2001; Quick et al., 2012; Ranade et al., 2014; Vilceanu and Stucky, 2010). However, conflicting results have been published regarding the precise role of some of these channels in mechanotransduction (Drew et al., 2004; Dubin et al., 2017). The only channel that has convincingly been shown to be required for mechanosensitivity of sensory neurons is PIEZO2. First, unlike the other aforementioned channels, PIEZO2 alone is sufficient to produce mechanotransduction currents when expressed in heterologous systems (Coste et al., 2010). Moreover, PIEZO2 knockout mice have severe deficits in proprioception (Woo et al., 2015) and in gentle touch perception (Ranade et al., 2014). Interestingly, PIEZO2 knockout mice do not seem to have problems detecting noxious mechanical stimuli and do develop hyperalgesia in the paw skin in the CFA model of inflammation (Ranade et al., 2014). However, PIEZO2 is expressed in almost 50% of all sensory neurons (Ranade et al., 2014), some of which express the heat-gated ion channel TRPV1 (Coste et al., 2010), suggesting that PIEZO2 is also present in some nociceptors. Using qPCR and immunohistochemistry, we show that PIEZO2 is indeed expressed in some nociceptors, namely, in CHRNA3^{+} neurons (Figures 7A and 7B). Moreover, the current-voltage relationship together with the voltage dependence of the inactivation kinetics and the GsMTX4-sensitivity (Figures 7C–7F), and, most important, the observation that siRNA-mediated knockdown of PIEZO2 renders NGF-treated CHRNA3^{+} neurons insensitive to mechanical stimuli (Figures 7G and 7H), suggests that the NGF-induced mechanotransduction currents in CHRNA3^{+} neurons are indeed mediated by PIEZO2. So why is it that PIEZO2 knockout mice do not have a pain phenotype? The simple answer is that Ranade et al. (2014) examined only cutaneous nociceptors, but as our data demonstrate, CHRNA3^{+} afferents do not innervate the skin. An important question that remains open, however, is why CHRNA3^{+} neurons are insensitive to mechanical stimuli under control conditions even though they express PIEZO2 (Figures 7A and 7B). At present we can only speculate about the possible mechanism. Our experiments, however, demonstrate that *de novo* gene transcription is required for the acquisition of mechanosensitivity (Figures 6A and 6B). Hence, as illustrated in Figure 7I, we propose that PIEZO2 is normally inhibited by a yet unknown protein and is released from this inhibition by another unidentified protein that is upregulated by NGF-TRKA-ERK1/2 signaling.

Conclusions

NGF signaling plays a central role in the development of mechanical hyperalgesia associated with inflammation. Despite the great efficacy of anti-NGF antibodies in alleviating pain, however, in 2010 all anti-NGF trials were placed on clinical hold for a period of almost 5 years, because of a high incidence of joint destruction in osteoarthritis patients receiving anti-NGF treatment and concerns regarding possible side effects on sympathetic neurons (Chang et al., 2016; Denk et al., 2017). Our work, especially the identification of a nociceptor subpopulation that is particularly sensitive to NGF and that predominantly innervates tissues in which anti-NGF therapy has proved extremely efficacious, provides an invaluable framework for future studies that aim to further unravel the mechanism underlying NGF-induced hyperalgesia and studies aimed at developing drugs that selectively block the effects of NGF in sensory neurons and would thus potentially have fewer side effects than currently available anti-NGF drugs.

EXPERIMENTAL PROCEDURES

Animals

CHRNA3-EGFP mice, official name Tg(Chrna3-EGFP)BZ135Gsat/Mmnc (RRID: MMRRC_000243-UNC), were obtained from the Mutant Mouse Resource & Research Center and were backcrossed to a C57BL/6J background. Additional information is provided in Supplemental Experimental Procedures. Mice were housed in the Interfacultary Biomedical Facility of Heidelberg University according to institutional guidelines. All animal experiments were carried out according to the German Animal Protection Law and with

permission of the Regierungspraesidium Karlsruhe (T-57/16). Retrograde tracing experiments were conducted at the University of Cambridge in accordance with the United Kingdom Animal (Scientific Procedures) Act 1986 Amendment Regulations 2012 under a Project License (70/7705) granted to E.S.S. by the Home Office; the University of Cambridge Animal Welfare Ethical Review Body also approved procedures.

Immunohistochemistry

A detailed description of the immunostaining protocols and the antibodies that were used is provided in Supplemental Experimental Procedures.

Cell Culture

DRG neurons from 8- to 12-week-old mice were cultured on glass coverslips coated with poly-L-lysine and laminin in DMEM-F12 medium supplemented with L-glutamine (2 μM), glucose (8 mg/mL), penicillin (200 U/mL)-streptomycin (200 μg/mL), and 5% fetal horse serum. Detailed information about the preparation of DRG cultures is provided in Supplemental Experimental Procedures.

Patch-Clamp Recordings

Whole-cell patch-clamp recordings were made at 20°C–24°C with an EPC10 amplifier (HEKA) and patch pipettes with a resistance of 2–4 MΩ. Neurons were clamped at a holding potential of −60 mV and stimulated with a series of mechanical stimuli in 1.6 μm increments with a fire-polished glass pipette (tip diameter 2–3 μm) that was positioned at an angle of 45° to the surface of the dish and moved with a velocity of 3.5 μm/ms by a piezo-driven micromanipulator (MM3A; Kleindiek Nanotechnik). Additional information is provided in Supplemental Experimental Procedures.

Retrograde Labeling

A detailed description of the retrograde labeling procedure is provided in Supplemental Experimental Procedures.

Single-Cell Electroporation and siRNA-Mediated Knockdown

CHRNA3$^+$ neurons were transfected with non-targeting siRNA (D-001810-01-05 ON-TARGETplus non-targeting siRNA; GE Healthcare) and PIEZO2-siRNA (L-163012-00-0005 ON-TARGETplus Mouse Piezo2 [667742] siRNA; SMARTpool), respectively, using single-cell electroporation. Details about the electroporation procedure are provided in Supplemental Experimental Procedures.

Reverse Transcription and Real-Time qPCR

mRNA expression levels of candidate mechanotransduction genes in CHRNA3$^+$ neurons were determined from samples containing 20 CHRNA3$^+$ neurons that were collected from DRG cultures by aspirating the cells into a patch-clamp pipette filled with 2–4 μL PBS containing 4 U/μL RNaseOUT (Thermo Fisher Scientific). cDNA synthesis was carried out directly on the sample using the Power SYBR Green Cells-to-CT Kit (Life Technologies) following the manufacturer's instructions. qPCRs were performed using FastStart Essential DNA Green Master (Roche) on a LightCycler 96 (Roche). Detailed information about primers and thermal cycle profile is provided in Supplemental Experimental Procedures.

Statistical Analysis

All statistical analyses were made using GraphPad Prism 5. The statistical tests that were used are mentioned in the figure legends and in the main text, respectively. To select the appropriate test, all datasets were tested for Gaussian distribution using the Kolmogorov-Smirnov test. N indicates the number of animals that were used; n indicates the number of cells. *p < 0.05, #p < 0.05, and §p < 0.05; **p < 0.01, ##p < 0.01, and §§p < 0.01; ***p < 0.001, ###p < 0.001, and §§§p < 0.001; ns, not significant (p > 0.05).

SUPPLEMENTAL INFORMATION

Supplemental Information includes Supplemental Experimental Procedures and four figures and can be found with this article online at https://doi.org/10.1016/j.celrep.2017.11.066.

ACKNOWLEDGMENTS

This study was supported by Deutsche Forschungsgemeinschaft (DFG) grants LE3210/1-1 and SFB1158/1 to S.G.L., DFG grant SFB1158/2 to P.A.H., Arthritis Research UK grant 20930 to G.C. and E.S.S., and Rosetrees Trust grant A1296 to J.R.F.H. and E.S.S. We thank Ms. Anke Niemann for technical assistance.

AUTHOR CONTRIBUTIONS

Conceptualization, S.G.L.; Methodology, E.S.S. and S.G.L.; Investigation, V.P., F.J.T., J.R.F.H., G.C., B.T., A.A., L.H., and P.S.; Writing, S.G.L.; Funding Acquisition, E.S.S., P.A.H., and S.G.L.; Resources, S.G.L.; Supervision, E.S.S., P.A.H., and S.G.L.

DECLARATION OF INTERESTS

The authors declare no competing interests.

Received: August 16, 2017
Revised: October 9, 2017
Accepted: November 14, 2017
Published: December 12, 2017

REFERENCES

Arcourt, A., Gorham, L., Dhandapani, R., Prato, V., Taberner, F.J., Wende, H., Gangadharan, V., Birchmeier, C., Heppenstall, P.A., and Lechner, S.G. (2017). Touch receptor-derived sensory information alleviates acute pain signaling and fine-tunes nociceptive reflex coordination. Neuron *93*, 179–193.

Averill, S., McMahon, S.B., Clary, D.O., Reichardt, L.F., and Priestley, J.V. (1995). Immunocytochemical localization of trkA receptors in chemically identified subgroups of adult rat sensory neurons. Eur. J. Neurosci. *7*, 1484–1494.

Bennett, D.L., Averill, S., Clary, D.O., Priestley, J.V., and McMahon, S.B. (1996). Postnatal changes in the expression of the trkA high-affinity NGF receptor in primary sensory neurons. Eur. J. Neurosci. *8*, 2204–2208.

Brenneis, C., Kistner, K., Puopolo, M., Segal, D., Roberson, D., Sisignano, M., Labocha, S., Ferreirós, N., Strominger, A., Cobos, E.J., et al. (2013). Phenotyping the function of TRPV1-expressing sensory neurons by targeted axonal silencing. J. Neurosci. *33*, 315–326.

Cavanaugh, D.J., Lee, H., Lo, L., Shields, S.D., Zylka, M.J., Basbaum, A.I., and Anderson, D.J. (2009). Distinct subsets of unmyelinated primary sensory fibers mediate behavioral responses to noxious thermal and mechanical stimuli. Proc. Natl. Acad. Sci. U S A *106*, 9075–9080.

Chang, D.S., Hsu, E., Hottinger, D.G., and Cohen, S.P. (2016). Anti-nerve growth factor in pain management: current evidence. J. Pain Res. *9*, 373–383.

Chen, W., Ye, D.-Y., Han, D.-J., Fu, G.-Q., Zeng, X., Lin, W., and Liang, Y. (2016). Elevated level of nerve growth factor in the bladder pain syndrome/interstitial cystitis: a meta-analysis. Springerplus *5*, 1072.

Christianson, J.A., Liang, R., Ustinova, E.E., Davis, B.M., Fraser, M.O., and Pezzone, M.A. (2007). Convergence of bladder and colon sensory innervation occurs at the primary afferent level. Pain *128*, 235–243.

Coste, B., Mathur, J., Schmidt, M., Earley, T.J., Ranade, S., Petrus, M.J., Dubin, A.E., and Patapoutian, A. (2010). Piezo1 and Piezo2 are essential components of distinct mechanically activated cation channels. Science *330*, 55–60.

da Silva Serra, I., Husson, Z., Bartlett, J.D., and Smith, E.S.J. (2016). Characterization of cutaneous and articular sensory neurons. Mol. Pain *12*, 12.

Denk, F., Bennett, D.L., and McMahon, S.B. (2017). Nerve growth factor and pain mechanisms. Annu. Rev. Neurosci. *40*, 307–325.

Di Castro, A., Drew, L.J., Wood, J.N., and Cesare, P. (2006). Modulation of sensory neuron mechanotransduction by PKC- and nerve growth factor-dependent pathways. Proc. Natl. Acad. Sci. U S A *103*, 4699–4704.

Drew, L.J., Wood, J.N., and Cesare, P. (2002). Distinct mechanosensitive properties of capsaicin-sensitive and -insensitive sensory neurons. J. Neurosci. *22*, RC228.

Drew, L.J., Rohrer, D.K., Price, M.P., Blaver, K.E., Cockayne, D.A., Cesare, P., and Wood, J.N. (2004). Acid-sensing ion channels ASIC2 and ASIC3 do not contribute to mechanically activated currents in mammalian sensory neurones. J. Physiol. *556*, 691–710.

Dubin, A.E., and Patapoutian, A. (2010). Nociceptors: the sensors of the pain pathway. J. Clin. Invest. *120*, 3760–3772.

Dubin, A.E., Murthy, S., Lewis, A.H., Brosse, L., Cahalan, S.M., Grandl, J., Coste, B., and Patapoutian, A. (2017). Endogenous Piezo1 can confound mechanically activated channel identification and characterization. Neuron *94*, 266–270.e3.

Dyck, P.J., Peroutka, S., Rask, C., Burton, E., Baker, M.K., Lehman, K.A., Gillen, D.A., Hokanson, J.L., and O'Brien, P.C. (1997). Intradermal recombinant human nerve growth factor induces pressure allodynia and lowered heat-pain threshold in humans. Neurology *48*, 501–505.

Fang, X., McMullan, S., Lawson, S.N., and Djouhri, L. (2005). Electrophysiological differences between nociceptive and non-nociceptive dorsal root ganglion neurones in the rat in vivo. J. Physiol. *565*, 927–943.

Feng, B., and Gebhart, G.F. (2011). Characterization of silent afferents in the pelvic and splanchnic innervations of the mouse colorectum. Am. J. Physiol. Gastrointest. Liver Physiol. *300*, G170–G180.

Feng, B., La, J.-H., Schwartz, E.S., Tanaka, T., McMurray, T.P., and Gebhart, G.F. (2012). Long-term sensitization of mechanosensitive and -insensitive afferents in mice with persistent colorectal hypersensitivity. Am. J. Physiol. Gastrointest. Liver Physiol. *302*, G676–G683.

Gebhart, G.F. (1999). Peripheral contributions to visceral hyperalgesia. Can. J. Gastroenterol. *13* (*Suppl. A*), 37A–41A.

Gold, M.S., and Gebhart, G.F. (2010). Nociceptor sensitization in pain pathogenesis. Nat. Med. *16*, 1248–1257.

Häbler, H.J., Jänig, W., and Koltzenburg, M. (1990). Activation of unmyelinated afferent fibres by mechanical stimuli and inflammation of the urinary bladder in the cat. J. Physiol. *425*, 545–562.

Hirth, M., Rukwied, R., Gromann, A., Turnquist, B., Weinkauf, B., Francke, K., Albrecht, P., Rice, F., Hägglöf, B., Ringkamp, M., et al. (2013). Nerve growth factor induces sensitization of nociceptors without evidence for increased intraepidermal nerve fiber density. Pain *154*, 2500–2511.

Hong, G.-S., Lee, B., Wee, J., Chun, H., Kim, H., Jung, J., Cha, J.Y., Riew, T.-R., Kim, G.H., Kim, I.-B., and Oh, U. (2016). Tentonin 3/TMEM150c confers distinct mechanosensitive currents in dorsal-root ganglion neurons with proprioceptive function. Neuron *91*, 107–118.

Hu, J., and Lewin, G.R. (2006). Mechanosensitive currents in the neurites of cultured mouse sensory neurones. J. Physiol. *577*, 815–828.

Knowlton, W.M., Palkar, R., Lippoldt, E.K., McCoy, D.D., Baluch, F., Chen, J., and McKemy, D.D. (2013). A sensory-labeled line for cold: TRPM8-expressing sensory neurons define the cellular basis for cold, cold pain, and cooling-mediated analgesia. J. Neurosci. *33*, 2837–2848.

Koerber, H.R., Druzinsky, R.E., and Mendell, L.M. (1988). Properties of somata of spinal dorsal root ganglion cells differ according to peripheral receptor innervated. J. Neurophysiol. *60*, 1584–1596.

Lechner, S.G., and Lewin, G.R. (2013). Hairy sensation. Physiology (Bethesda) *28*, 142–150.

Lechner, S.G., Frenzel, H., Wang, R., and Lewin, G.R. (2009). Developmental waves of mechanosensitivity acquisition in sensory neuron subtypes during embryonic development. EMBO J. *28*, 1479–1491.

Lee, Y.-J., Zachrisson, O., Tonge, D.A., and McNaughton, P.A. (2002). Upregulation of bradykinin B2 receptor expression by neurotrophic factors and nerve injury in mouse sensory neurons. Mol. Cell. Neurosci. *19*, 186–200.

Lewin, G.R., and Moshourab, R. (2004). Mechanosensation and pain. J. Neurobiol. *61*, 30–44.

Lewin, G.R., Ritter, A.M., and Mendell, L.M. (1993). Nerve growth factor-induced hyperalgesia in the neonatal and adult rat. J. Neurosci. *13*, 2136–2148.

Lewin, G.R., Lechner, S.G., and Smith, E.S.J. (2014). Nerve growth factor and nociception: from experimental embryology to new analgesic therapy. Handb. Exp. Pharmacol. *220*, 251–282.

Luo, W., Wickramasinghe, S.R., Savitt, J.M., Griffin, J.W., Dawson, T.M., and Ginty, D.D. (2007). A hierarchical NGF signaling cascade controls Ret-dependent and Ret-independent events during development of nonpeptidergic DRG neurons. Neuron *54*, 739–754.

McCarter, G.C., Reichling, D.B., and Levine, J.D. (1999). Mechanical transduction by rat dorsal root ganglion neurons in vitro. Neurosci. Lett. *273*, 179–182.

Meyer, R.A., Davis, K.D., Cohen, R.H., Treede, R.D., and Campbell, J.N. (1991). Mechanically insensitive afferents (MIAs) in cutaneous nerves of monkey. Brain Res. *561*, 252–261.

Michaelis, M., Häbler, H.J., and Jäenig, W. (1996). Silent afferents: a separate class of primary afferents? Clin. Exp. Pharmacol. Physiol. *23*, 99–105.

Molliver, D.C., and Snider, W.D. (1997). Nerve growth factor receptor TrkA is down-regulated during postnatal development by a subset of dorsal root ganglion neurons. J. Comp. Neurol. *381*, 428–438.

Molliver, D.C., Wright, D.E., Leitner, M.L., Parsadanian, A.S., Doster, K., Wen, D., Yan, Q., and Snider, W.D. (1997). IB4-binding DRG neurons switch from NGF to GDNF dependence in early postnatal life. Neuron *19*, 849–861.

Pezet, S., and McMahon, S.B. (2006). Neurotrophins: mediators and modulators of pain. Annu. Rev. Neurosci. *29*, 507–538.

Price, M.P., Lewin, G.R., McIlwrath, S.L., Cheng, C., Xie, J., Heppenstall, P.A., Stucky, C.L., Mannsfeldt, A.G., Brennan, T.J., Drummond, H.A., et al. (2000). The mammalian sodium channel BNC1 is required for normal touch sensation. Nature *407*, 1007–1011.

Price, M.P., McIlwrath, S.L., Xie, J., Cheng, C., Qiao, J., Tarr, D.E., Sluka, K.A., Brennan, T.J., Lewin, G.R., and Welsh, M.J. (2001). The DRASIC cation channel contributes to the detection of cutaneous touch and acid stimuli in mice. Neuron *32*, 1071–1083.

Quick, K., Zhao, J., Eijkelkamp, N., Linley, J.E., Rugiero, F., Cox, J.J., Raouf, R., Gringhuis, M., Sexton, J.E., Abramowitz, J., et al. (2012). TRPC3 and TRPC6 are essential for normal mechanotransduction in subsets of sensory neurons and cochlear hair cells. Open Biol. *2*, 120068.

Ranade, S.S., Woo, S.-H., Dubin, A.E., Moshourab, R.A., Wetzel, C., Petrus, M., Mathur, J., Bégay, V., Coste, B., Mainquist, J., et al. (2014). Piezo2 is the major transducer of mechanical forces for touch sensation in mice. Nature *516*, 121–125.

Rukwied, R., Mayer, A., Kluschina, O., Obreja, O., Schley, M., and Schmelz, M. (2010). NGF induces non-inflammatory localized and lasting mechanical and thermal hypersensitivity in human skin. Pain *148*, 407–413.

Schaible, H.G., and Schmidt, R.F. (1985). Effects of an experimental arthritis on the sensory properties of fine articular afferent units. J. Neurophysiol. *54*, 1109–1122.

Schaible, H.G., and Schmidt, R.F. (1988). Time course of mechanosensitivity changes in articular afferents during a developing experimental arthritis. J. Neurophysiol. *60*, 2180–2195.

Schmidt, R., Schmelz, M., Forster, C., Ringkamp, M., Torebjörk, E., and Handwerker, H. (1995). Novel classes of responsive and unresponsive C nociceptors in human skin. J. Neurosci. *15*, 333–341.

Schrenk-Siemens, K., Wende, H., Prato, V., Song, K., Rostock, C., Loewer, A., Utikal, J., Lewin, G.R., Lechner, S.G., and Siemens, J. (2015). PIEZO2 is required for mechanotransduction in human stem cell-derived touch receptors. Nat. Neurosci. *18*, 10–16.

Vilceanu, D., and Stucky, C.L. (2010). TRPA1 mediates mechanical currents in the plasma membrane of mouse sensory neurons. PLoS ONE *5*, e12177.

Wang, F., Knutson, K., Alcaino, C., Linden, D.R., Gibbons, S.J., Kashyap, P., Grover, M., Oeckler, R., Gottlieb, P.A., Li, H.J., et al. (2017). Mechanosensitive ion channel Piezo2 is important for enterochromaffin cell response to mechanical forces. J. Physiol. *595*, 79–91.

Wetzel, C., Hu, J., Riethmacher, D., Benckendorff, A., Harder, L., Eilers, A., Moshourab, R., Kozlenkov, A., Labuz, D., Caspani, O., et al. (2007). A stomatin-domain protein essential for touch sensation in the mouse. Nature *445*, 206–209.

Weyer, A.D., Zappia, K.J., Garrison, S.R., O'Hara, C.L., Dodge, A.K., and Stucky, C.L. (2016). Nociceptor Sensitization Depends on Age and Pain Chronicity(1,2,3). eNeuro *3*, 3.

Woo, S.-H., Lukacs, V., de Nooij, J.C., Zaytseva, D., Criddle, C.R., Francisco, A., Jessell, T.M., Wilkinson, K.A., and Patapoutian, A. (2015). Piezo2 is the principal mechanotransduction channel for proprioception. Nat. Neurosci. *18*, 1756–1762.

Woolf, C.J., Safieh-Garabedian, B., Ma, Q.P., Crilly, P., and Winter, J. (1994). Nerve growth factor contributes to the generation of inflammatory sensory hypersensitivity. Neuroscience *62*, 327–331.

Cell Reports, Volume *21*

Supplemental Information

Functional and Molecular Characterization of Mechanoinsensitive "Silent" Nociceptors

Vincenzo Prato, Francisco J. Taberner, James R.F. Hockley, Gerard Callejo, Alice Arcourt, Bassim Tazir, Leonie Hammer, Paulina Schad, Paul A. Heppenstall, Ewan S. Smith, and Stefan G. Lechner

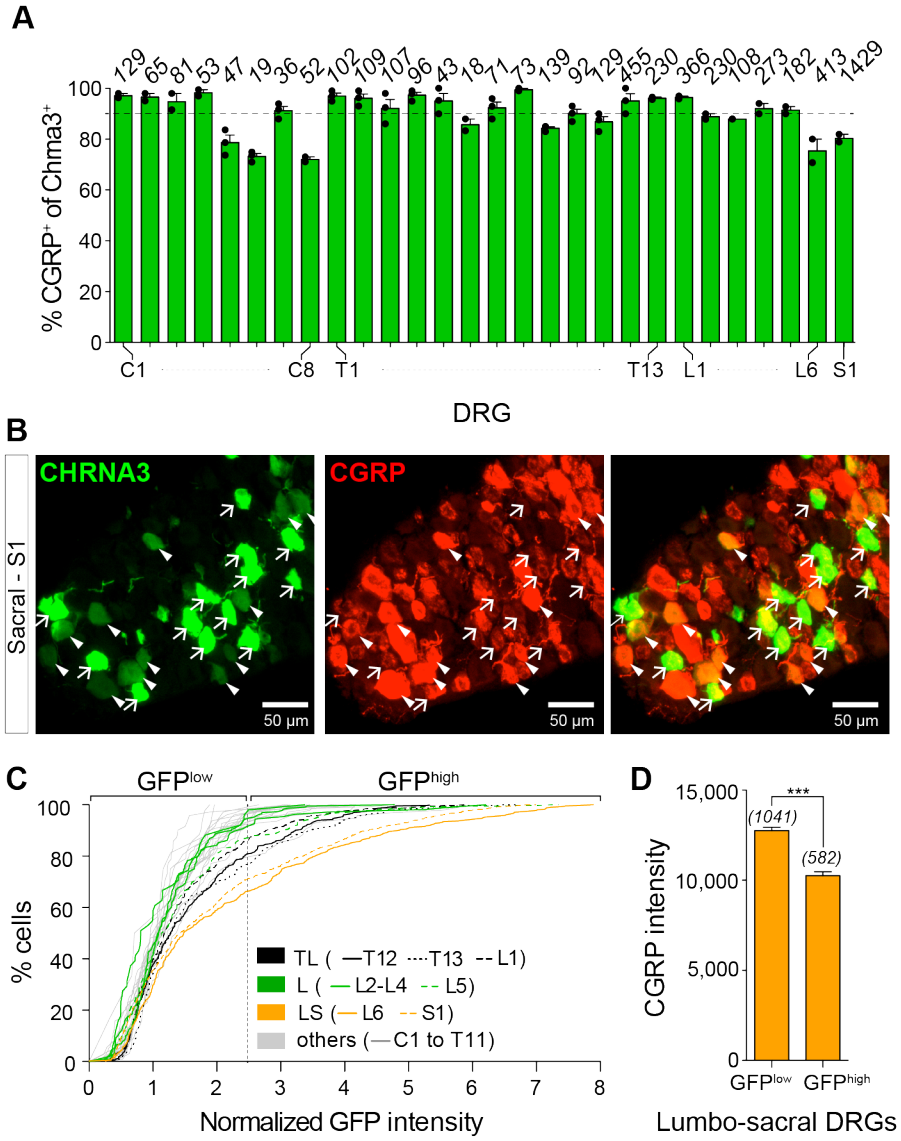

Figure S1, related to Figure 2, Lumbosacral DRGs comprise two populations of CHRNA3$^+$ neurons

(A) Bar graph showing the percentage of CHRNA3$^+$ neurons that express CGRP. Bars represent means ± s.e.m. (N = 2 - 3 DRGs from 2 - 3 mice) and individual percentages of each analyzed DRG are shown as black circles. Numbers above the bars represent the total number of analyzed CHRNA3$^+$ neurons.

(B) Representative images showing CGRP expression in GFP^{low} (arrowheads) and GFP^{high} (arrows) CHRNA3$^+$ neurons.

(C) GFP intensities from individual DRGs and different experiments were fitted with a Gaussian function and with the sum of two Gaussians. The best fitting model was determined using the extra sum-of-squares F test of Graphpad Prism 5. C1 - T11 and L2 - L5 GFP intensity distributions were best fitted with a single Gaussian and with the sum of two Gaussians for T12 - L1 and L6 - S1 DRGs. The graph shows the cumulative distribution of GFP intensities normalized to the mean intensity value of the GFP^{low} population of the indicated DRGs.

(D) Bar graph showing that GFP^{low} neurons express higher levels of CGRP. Bars represent means ± s.e.m.. The numbers of analyzed cells are indicated above the bars. ***, P<0.001, Student's T-test.

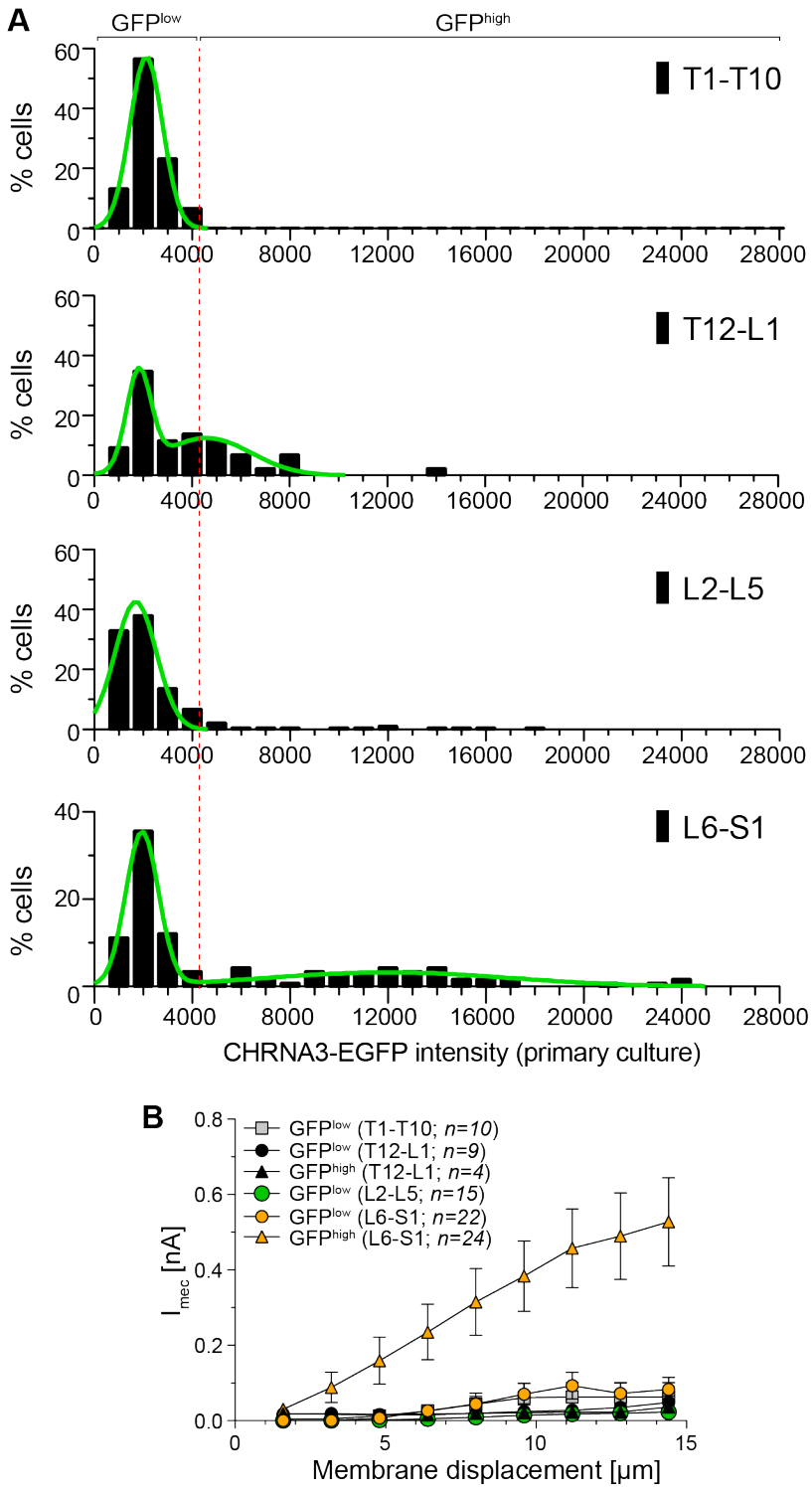

Figure S2, related to Figure 2, GFP^{low} and GFP^{high} CHRNA3^{+} neurons have different functional properties.

(A) Frequency distribution plot of GFP-intensities showing that GFP^{low} and GFP^{high} neurons can also be distinguished by means of the endogenous GFP signals in DRG cultures. The 90th percentile of the L2-L5 GFP-intensity distribution was used as the cut-off to distinguish between GFP^{low} and GFP^{high} neurons (vertical dashed line).

(B) Mean ± s.e.m. amplitudes of mechanically evoked currents in CHRNA3^{+} GFP^{low} and GFP^{high} neurons from the indicated spinal segments are shown as a function of membrane displacement. Note that only GFP^{high} neurons from L6-S1 exhibit mechanotransduction currents.

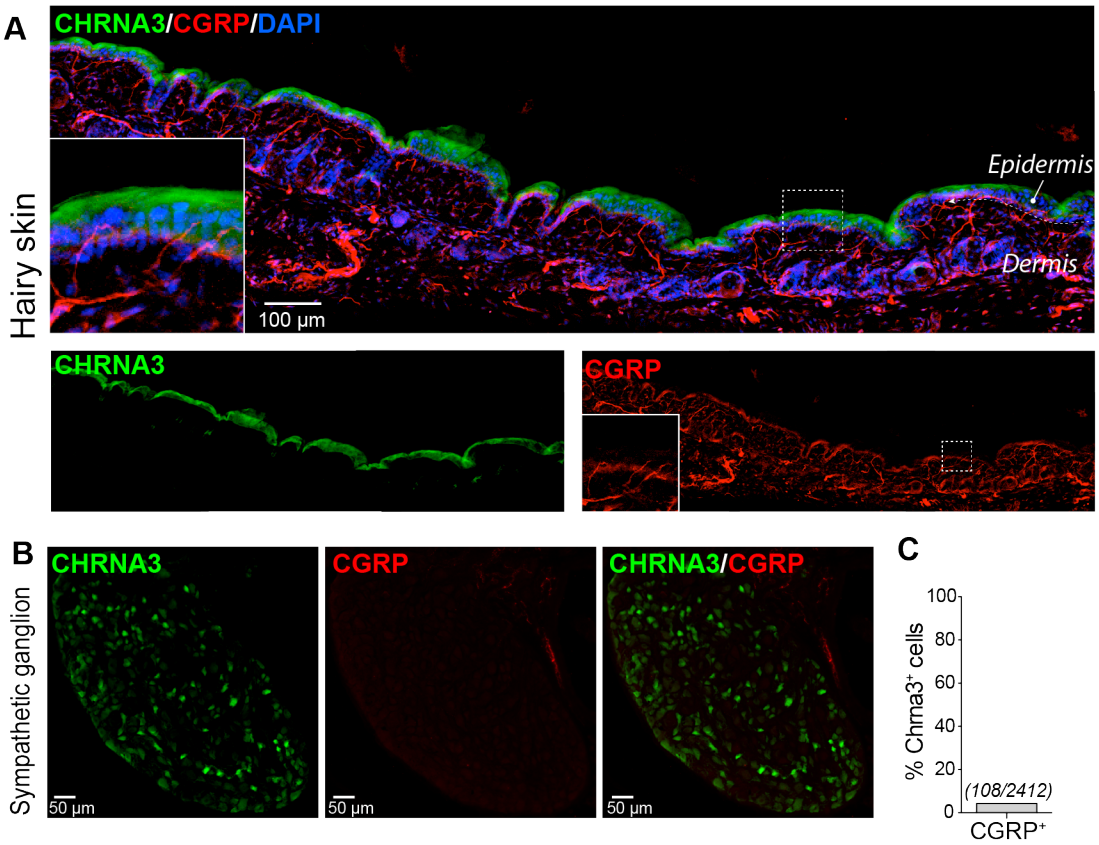

Figure S3, related to Figure 3, CHRNA3$^+$ afferents do not innervate hairy skin

(A) Immunostainings showing that CHRNA3$^+$ afferents do not innervate the hairy skin.

(B) Immunostaining showing that some neurons in sympathetic ganglia also express CHRNA3; these neurons do however not express CGRP.

(C) Bar graph showing the percentage of CHRNA3$^+$ sympathetic neurons that express CGRP.

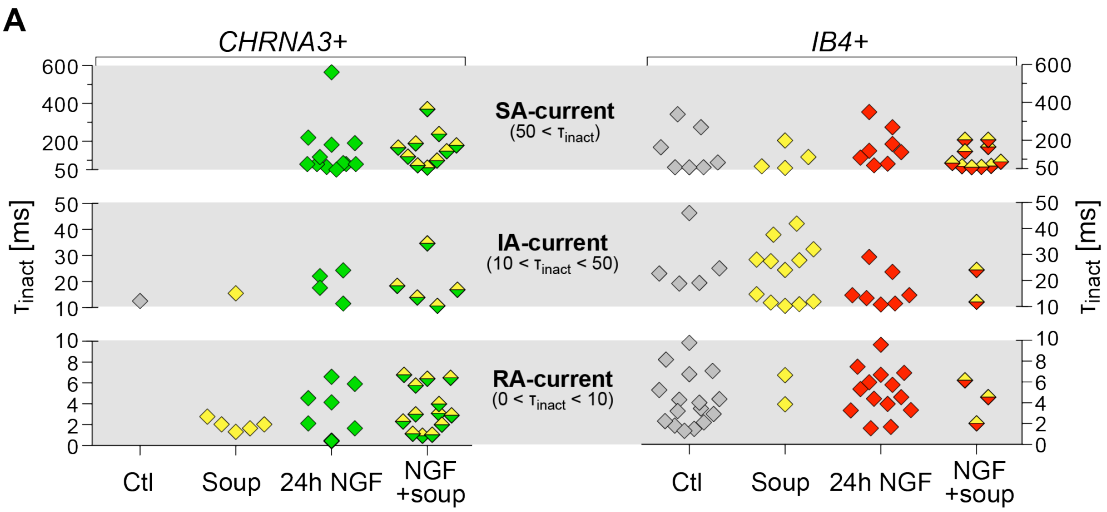

Figure S4, related to Figure 5. Inactivation time constants of mechanotransduction currents.
(A) Same data as in Figure 5C and F, but shown as a scatter dot plot of inactivation time constants (τ_{inact}) of the mechanotransduction currents recorded from CHRNA3$^+$ neurons (left panel) and IB4$^+$ neurons (right panel) in the indicated conditions. Each data point shows the τ_{inact} of a single neuron.

Supplemental Experimental Procedures

Animals

CHRNA3-EGFP mice, official name Tg(Chrna3-EGFP)BZ135Gsat/Mmnc (RRID:MMRRC_000243-UNC) were obtained from the Mutant Mouse Resource & Research Center (MMRRC) and were backcrossed to a C57Bl/6J background. Mice were housed in the Interfacultary Biomedical Facility of Heidelberg University according to institutional guidelines. All animal experiments were carried out according to the German Animal Protection Law and with permission of the Regierungspraesidium Karlsruhe (T-57/16). Retrograde tracing experiments were conducted at the University of Cambridge in accordance with the United Kingdom Animal (Scientific Procedures) Act 1986 Amendment Regulations 2012 under a Project License (70/7705) granted to E. St. J. S. by the Home Office; the University of Cambridge Animal Welfare Ethical Review Body also approved procedures. For all experiments both male and female 8-12 weeks old mice were used.

Immnuohistochemistry

DRGs were dissected in ice-cooled PBS, fixed with 4% PFA for 30 min at 4 °C and incubated overnight in 30 % sucrose at 4°C. DRGs were then embedded in Tissue-Tek O.C.T compound and cut into 16 µm cryo-sections. After drying, sections were incubated in 50 mM Glycine for 20 min, washed twice with PBST (0.2 %), blocked with PBST (0.2 %) + 10% donkey serum + 1% BSA and then incubated with primary antibodies for 1 h at room temperature. Primary antibodies were diluted in PBST (0.2 %) + 10 % donkey serum. Sections were then washed four times with PBST (0.2 %), subsequently incubated with secondary antibodies for 1 h at RT, washed with PBST four times, dried and mounted with fluorogel (Fluoprobes).

Glabrous skin, hairy skin, urinary bladder, distal colon, gastrocnemius muscle and spinal cord samples were dissected in cold PBS and fixed with Zambonis fixative for 2 h at RT, washed four times and incubated in 30 % sucrose at 4 °C overnight. Knee joints were fixed with Zambonis fixative over night. Prior to cutting, knee joints were decalcified by submerging the samples in PBS + 10 % EDTA for 7 days (PBS/EDTA was replaced every day). For the preparation of tissue sections, samples were embedded in Tissue-Tek, frozen with liquid nitrogen and cut into 50 µm cryo-sections. After drying, sections were incubated in 50 mM Glycine for 45 min, washed twice with PBST (0.2 %), blocked 1 h with PBST (0.2 %) + 10 % donkey serum + 1 % BSA and then incubated with primary antibodies overnight at 4°C. Primary antibodies were diluted in PBST (0.2 %) + 10 % donkey serum + 1 % BSA. Sections were then washed several times with PBST (0.2 %), subsequently incubated for 4 hours with secondary antibodies in PBST (0.2 %) + 10% donkey serum + 1% BSA at room temperature, washed with PBST (0.2%) several times, dried and mounted with fluorogel (Fluoprobes).

Antibodies

The following primary antibodies were used: rat anti-GFP (Nacalai tesque, #04404-84, 1:3000; RRID:AB_10013361), mouse anti-Nefh (Sigma-Aldrich, N0142, 1:600, RRID:AB_477257), goat anti-TrkA (R&D, AF1056, 1:200, RRID:AB_2283049), rabbit anti-CGRP (ImmunoStar, 1:200, RRID:AB_572217), rabbit anti-PIEZO2 (Novus, 1:100, RRID:AB_11008402) (Florez-Paz et al., 2016; Narayanan et al., 2016), and Isolectin GS-IB4-Alexa Fluor® 568 Conjugate (Life technologies, 3 µg/ml). Secondary antibodies were AlexaFluor-488 donkey anti-rat (Life technologies, AF21208, 1:500, RRID:AB_2535794), AlexaFluor-594 donkey anti-mouse (Life technologies, AF21203 1:500, RRID:AB_2535789), AlexaFluor-633 donkey anti-goat (Life technologies, A21082, 1:500, RRID:AB_10562400), AlexaFluor-594 donkey anti-rabbit (Life technologies, A2107, 1:500, RRID:AB_141637).

Cell culture

8-12 weeks old mice were killed by placing them in a CO_2-filled chamber for 2–4 min followed by cervical dislocation and DRGs were collected in Ca^{2+} and Mg^{2+}-free PBS. DRGs were subsequently treated with collagenase IV for 30 minutes (1 mg/ml, Sigma) and with trypsin (0.05 %, Life Technologies) for a further 30 minutes, at 37 °C. Digested DRG's were washed twice with growth medium [DMEM-F12 (Invitrogen) supplemented with L-glutamine (2 µM, Sigma), glucose (8 mg/ml, Sigma), penicillin (200 U/ml)–streptomycin (200 µg/ml) (both Life Technologies) 5 % fetal horse serum (Life Technologies)], triturated using fire-polished Pasteur pipettes and plated in a droplet of growth medium on a glass coverslip precoated with poly-L-lysine (20 µg/cm², Sigma) and laminin (4µg/cm², Life Technologies). To allow neurons to adhere, coverslips were kept for 3 - 4 hours at 37 °C in a humidified 5 % incubator before being flooded with fresh growth medium. Cultures were used for patch-clamp experiments on the next day.

Patch-clamp recordings

Whole cell patch clamp recordings were made at room temperature (20-24°C). Patch pipettes with a tip resistance of 2-4 MΩ were pulled (Flaming-Brown puller, Sutter Instruments, Novato, CA, USA) from borosilicate glass capillaries (BF150-86-10, Sutter Instrument), filled with a solution consisting of 110 mM KCl, 10 mM NaCl, 1 mM $MgCl_2$, 1 mM EGTA, 10 mM HEPES, 2 mM guanosine 5'-triphosphate (GTP) and 2 mM adenosine 5'-triphosphate (ATP) adjusted to pH 7.3 with KOH. The bathing solution contained 140 mM NaCl, 4 mM KCl, 2 mM $CaCl_2$, 1 mM $MgCl_2$, 4 mM glucose, 10 mM HEPES, adjusted to pH 7.4 with NaOH. Drugs were applied with a gravity driven multi-barrel perfusion system (Valvelink8.2, Automate Scientific). All recordings were made using an EPC-10 amplifier (HEKA, Lambrecht, Germany) in combination with Patchmaster© and Fitmaster© software (HEKA). Pipette and membrane capacitance were compensated using the auto function of Patchmaster and series resistance was compensated by 70 % to minimize voltage errors.

Mechanically activated currents were recorded in the whole-cell patch-clamp configuration. Neurons were clamped to a holding potential of -60 mV and stimulated with a series of mechanical stimuli in 1.6 µm increments with a fire-polished glass pipette (tip diameter 2-3µm) that was positioned at an angle of 45° to the surface of the dish and moved with a velocity of 3.5µm/ms by a piezo based micromanipulator called nanomotor© (MM3A, Kleindiek Nanotechnik, Reutlingen, Germany). The evoked whole cell currents were recorded with a sampling frequency of 200 kHz. Mechanotransduction current inactivation was fitted with a single exponential function ($C_1+C_2*\exp(-(t-t_0)/\tau_{inact})$, where C1 and C2 are constants, t is time and τ_{inact} is the inactivation time constant. Currents with a $\tau_{inact} < 10$ ms were classified as RA-type currents, currents with τ_{inact} between 10 and 50 ms as IA-type currents and currents that with $\tau_{inact} > 50$ ms as SA-type currents (Lechner and Lewin, 2009). For classification of sensory neurons, action potentials were recorded in current-clamp mode and evoked by repetitive 80 ms current injections increasing from 40 pA to 800 pA in increments of 40 pA.

Retrograde labeling

Retrograde labeling of sensory neurons innervating the knee was performed in CHRNA3-EGFP (male, 11-15 weeks old) mice as described previously (da Silva Serra et al., 2016) using Fast Blue (FB; 2 % in saline, Polysciences Gmbh, Germany). Mice were anaesthetized by an intra-peritoneal injection of ketamine (100 mg/kg) and xylazine (10 mg/kg). Once no withdrawal reflexes were observed, mice (n = 4) received FB intraarticular injections in both hind limb knees (1.5 µl). Injections were performed using a 10 µl Hamilton syringe and a 30G needle. Retrograde labeling of sensory neurons innervating visceral organs (bladder and colon) was also performed in CHRNA3-EGFP mice (male, 11-15 weeks old) using FB as previously described (Hockley et al., 2014, 2016, 2017). In brief, mice were anaesthetized using isofluorane (4 % induction / 1.5 % maintenance) and a mid-line laparotomy performed to reveal the visceral organs. FB was injected into the wall of the distal colon (n = 3, 6 injections per animal, total volume ~2 µl), and in separate animals, the bladder (n = 3, single injection per animal, ~5 µl), before closure of the laparotomy and allowing the animal to recover. Post-operative care (glucose-enriched soft diet) and analgesia (buprenorphine 0.05-0.1 mg/kg subcutaneously) was provided for 5 days. After 7 days, for knee-labeled mice, and 14 days, for colon- and bladder-labeled mice, animals were anaesthetized with sodium pentobarbital (140 mg/kg, intraperitoneally) and transcardially perfused with saline (0.9 % NaCl) followed by 4 % PFA in PBS. Lumbar (L3-L4) DRG were dissected from knee-labeled mice and thoracolumbar (T13) and lumbosacral (S1) DRG were dissected from colon- and bladder-labelled mice. All DRG dissected were post-fixed for 30 mins in 4 % PFA, washed in PBS and cryoprotected in 30 % sucrose overnight.

Single cell electroporation and siRNA-mediated knockdown

$CHRNA3^+$ neurons were transfected with non-targeting siRNA (, D-001810-01-05 ON-TARGETplus Non-targeting siRNA, GE-Healthcare) and PIEZO2-siRNA (L-163012-00-0005 ON-TARGETplus Mouse Piezo2 (667742) siRNA – SMARTpool), respectively, using single cell electroporation (Bestman et al., 2006; Haas et al., 2001). 4 hours after plating, single $CHRNA3^+$ neurons were approached with 1.5 MOhm patch pipettes filled with 5 µM siGLO RED (GE-Healthcare) transfection indicator and 500 nM non-targeting siRNA or 500 nM PIEZO2-siRNA diluted in intracellular patch-clamp buffer (see above). The patch clamp electrode and the bath electrode were connected to an isolated pulse stimulator (A-M Systems, Model 2100). As soon as the patch pipette touched the cell surface, 2 consecutive trains of square shaped electrical pulses (amplitude = 2.5 V, pulse duration = 2 ms, frequency 200 Hz, train duration 500 ms) were applied to electroporate the membrane and to drive siGLO and siRNA into the cell. After transfection, cultures were kept in the presence of 50ng/ml NGF for 72 h at 37 °C in a humidified 5 % incubator prior to cell collection or patch clamp recordings.

Patch-clamp recording from siRNA-transfected neurons were performed as described above. The efficiency of PIEZO2 knock-down was tested by qPCR. To this end samples of five transfected neurons were aspirated into the patch pipette and processed as described below.

Reverse transcription and quantitative real-time PCR
mRNA expression levels of candidate mechanotransduction genes in CHRNA3+ neurons were determined as follows. Samples containing 20 CHRNA3^{+} neurons were collected from DRG cultures by aspirating the cells into a patch clamp pipette with a tip diameter of 25 µm, filled with 2-4µl PBS containing 4 U/µl RNAseOUT (Thermofisher). For each gene three to four samples (one sample per mouse from a total of 3 - 4 CHRNA3-EGFP mice) were collected. cDNA synthesis was carried out directly on the sample using the Power SYBR® Green Cells-to-CT™ Kit (Life Technologies) following the manufacturers instructions. qPCR reactions were set up using FastStart Essential DNA Green Master (Roche) by adding 4 µL of the obtained cDNA as template and the following primer pairs at a concentriation of 250 nM:

ASIC2_ FWD	5'-GGCTTACTGGCAGAAAAGGA-3'
ASIC2_ REV	5'-CTTGCTGGGGATCTTTACCA-3'
ASIC3_ FWD	5'-GAGACATTGGGGGACAGATG-3'
ASIC3_ REV	5'-CCCCAGGACTCTGTCTTGAA-3'
TRPA1_FWD	5'-CACAGACCGACTAGATGAAGAAGG-3'
TRPA1_REV	5'-GGGCAATATGCAGAAAGGAGG-3'
TRPC3_FWD	5'-GGAGAGCGATCTGAGCGAAGT-3'
TRPC3_REV	5'-GGGAGCCATTTGTCTCTAGCA-3'
TRPC6_ FWD	5'-ACTACATTGGCGCAAAACAGAA-3'
TRPC6_ REV	5'-AGAAAGACCAAAGATAGCCCAGAA-3'
TMEM150c_ FWD	5'-TAGCCCTCGTGGTAGCTGTT-3'
TMEM150c_ REV	5'-CATCGTTTGTGAGCTGGAAA-3'
PIEZO2_ FWD	5'-TTCAACCAGGGGTCCCAAGC-3'
PIEZO2_ REV	5'-TCCCAATTACAAGGACAACAGATGC-3'
GAPDH- FWD	5'-GCATGGCCTTCCGTGTTC-3'
GAPDH- REV	5'-GTAGCCCAAGATGCCCTTCA-3'

qPCR reactions were performed in a LightCycler 96 (Roche) with a thermal cycler profile as follows: 10 min preincubation step at 95°C followed by 40 cycles of PCR with a 10 second denaturing cycle at 95°C, followed by 10 seconds of annealing at 60ºC and 10 seconds extension at 72°C.

Supplemental References

Bestman, J.E., Ewald, R.C., Chiu, S.-L., and Cline, H.T. (2006). In vivo single-cell electroporation for transfer of DNA and macromolecules. Nat. Protoc. *1*, 1267–1272.

Florez-Paz, D., Bali, K.K., Kuner, R., and Gomis, A. (2016). A critical role for Piezo2 channels in the mechanotransduction of mouse proprioceptive neurons. Sci. Rep. *6*, 25923.

Haas, K., Sin, W.-C., Javaherian, A., Li, Z., and Cline, H.T. (2001). Single-Cell Electroporationfor Gene Transfer In Vivo. Neuron *29*, 583–591.

Hockley, J.R.F., Boundouki, G., Cibert-Goton, V., McGuire, C., Yip, P.K., Chan, C., Tranter, M., Wood, J.N., Nassar, M.A., Blackshaw, L.A., et al. (2014). Multiple roles for NaV1.9 in the activation of visceral afferents by noxious inflammatory, mechanical, and human disease-derived stimuli. Pain *155*, 1962–1975.

Hockley, J.R.F., Tranter, M.M., McGuire, C., Boundouki, G., Cibert-Goton, V., Thaha, M.A., Blackshaw, L.A., Michael, G.J., Baker, M.D., Knowles, C.H., et al. (2016). P2Y Receptors Sensitize Mouse and Human Colonic Nociceptors. J. Neurosci. Off. J. Soc. Neurosci. *36*, 2364–2376.

Hockley, J.R.F., González-Cano, R., McMurray, S., Tejada-Giraldez, M.A., McGuire, C., Torres, A., Wilbrey, A.L., Cibert-Goton, V., Nieto, F.R., Pitcher, T., et al. (2017). Visceral and somatic pain modalities reveal NaV 1.7-independent visceral nociceptive pathways. J. Physiol. *595*, 2661–2679.

Lechner, S.G., and Lewin, G.R. (2009). Peripheral sensitisation of nociceptors via G-protein-dependent potentiation of mechanotransduction currents. J. Physiol. *587*, 3493–3503.

Narayanan, P., Sondermann, J., Rouwette, T., Karaca, S., Urlaub, H., Mitkovski, M., Gomez-Varela, D., and Schmidt, M. (2016). Native Piezo2 Interactomics Identifies Pericentrin as a Novel Regulator of Piezo2 in Somatosensory Neurons. J. Proteome Res. *15*, 2676–2687.

da Silva Serra, I., Husson, Z., Bartlett, J.D., and Smith, E.S.J. (2016). Characterization of cutaneous and articular sensory neurons. Mol. Pain *12*.